The 4DEnVar-based land weakly coupled data assimilation system for E3SM version 2

Pengfei Shi[1], L. Ruby Leung[1], Bin Wang[2], Kai Zhang[1], Samson M. Hagos[1], and Shixuan Zhang[1]

[1]Atmospheric Sciences and Global Change Division, Pacific Northwest National Laboratory, Richland, Washington, USA

[2]State Key Laboratory of Numerical Modeling for Atmospheric Sciences and Geophysical Fluid Dynamics (LASG), Institute of Atmospheric Physics, Chinese Academy of Sciences, Beijing, China

Correspondence: L. Ruby Leung (Ruby.Leung@pnnl.gov) and Pengfei Shi (pengfei.shi@pnnl.gov)

Abstract. A new weakly coupled land data assimilation (WCLDA) system based on the four-dimensional ensemble variational (4DEnVar) method is developed and applied to the fully coupled Energy Exascale Earth System Model version 2 (E3SMv2). The dimension-reduced projection four-dimensional variational (DRP-4DVar) method is employed to implement 4DVar using the ensemble technique instead of the adjoint technique. With an initial interest in providing initial conditions for decadal climate predictions, monthly mean anomalies of soil moisture and temperature analyses from the Global Land Data Assimilation System (GLDAS) reanalysis are assimilated into the land component of E3SMv2 within the coupled modeling framework with a one-month assimilation window from 1980 to 2016. The coupled assimilation experiment is evaluated using multiple metrics, including the cost function, assimilation efficiency index, correlation, root mean square error (RMSE) and bias, and compared with a control simulation without land data assimilation. The WCLDA system yields improved simulation of soil moisture and temperature compared with the control simulation, with improvements found throughout the soil layers and in many regions of the global land. In terms of both soil moisture and temperature, the assimilation experiment outperforms the control simulation with reduced RMSE and enhanced temporal correlation in many regions, especially in South America, Central Africa, Australia, and large parts of Eurasia. Furthermore, significant improvements are also found in reproducing the time evolution of the 2012 U.S. Midwest drought, highlighting the crucial role of land surface in drought lifecycle. The WCLDA system is intended to be a foundational resource for research to investigate land-derived climate predictability.

删除了：land

删除了：LCDA

删除了：M

删除了：

删除了：a global land reanalysis product

删除了：

删除了： along the coupled model trajectory

删除了：LCDA

删除了：

删除了：Furthermore, significant improvements are also found in reproducing the time evolution of the 2012 U.S. Midwest drought, highlighting the crucial role of land surface in drought lifecycle. The LCDA system is intended to be a foundational resource to investigate land-derived climate predictability for future prediction research by the E3SM community.

1 Introduction

The intrinsic chaos of the atmosphere limits traditional weather forecasting to roughly two weeks (Simmons and Hollingsworth, 2002). The feasibility of atmospheric predictability beyond two weeks lies with the interactions of the atmosphere with slowly varying components of the Earth system such as the ocean or land surface, or from predictable external forcing (Guo et al., 2012). Climate prediction can therefore be conceptually divided into both an initial value and a forced boundary value problem (Collins and Allen, 2002; Conil et al., 2007). One of the biggest technical challenges for improving the quality of climate predictions is the initialization of coupled models from observations (Taylor et al., 2012).

Much work has been devoted to initializing climate system models for practicable decadal climate predictions (DCPs). These models couple various components, such as models of the atmosphere, land surface, ocean, sea ice, and so on. Due to their much higher complexity, coupled models are often more susceptible to initial conditions (ICs) than their individual model components, underscoring the importance of dedicated data assimilation (DA) (Sakaguchi et al., 2012). The capability of DA methods is essential to incorporate available observations into the components of coupled model and produce the optimal estimate of ICs to improve DCPs. The initialization for DCPs uses uncoupled DA and coupled data assimilation (CDA) methods. Uncoupled DA performs DA under the framework of an individual component model (e.g., standalone land surface model forced by atmospheric observations or reanalysis data rather than coupled with an atmospheric model), and then the uncoupled DA analyses from different individual components are combined to form the ICs of a coupled model (Zhang et al., 2020). For example, most existing reanalysis data were produced using uncoupled DA approaches, and these reanalysis datasets are then directly used to initialize DCPs in some studies (Du et al., 2012; Bellucci et al., 2013). However, such uncoupled DA often exhibits poor consistency among the ICs of different component models, and eventually produces low prediction skills (Balmaseda et al., 2009; Boer et al., 2016; Ardilouze et al., 2017).

To obtain balanced multi-component ICs in coupled models, recent studies focus on the development of CDA methods under the coupled modeling framework (Penny and Hamill, 2017; He et al., 2020a). The purpose of CDA is to produce balanced and coherent ICs for all components within the climate system by incorporating observational information from one or more components in the coupled

model, providing great potential for improving seamless climate predictions (Dee et al., 2014). Some studies underscore the superior advantages of CDA over traditional uncoupled DA methods (Lea et al., 2015; Zhang et al., 2005). CDA methods are categorized into two main types: weakly coupled data assimilation (WCDA) and strongly coupled data assimilation (SCDA). WCDA assimilates the observations or existing reanalysis into the respective component of the coupled model and then transfers the observational information to the other components through the coupled model integration (He et al., 2020b; Zhang et al., 2020). Considering that sequential DA encompasses both the analysis and the forecast steps, WCDA allows no direct influence of observations from a single component to other components in the analysis step as the cross-component background error covariances are not used, but coupling in the forecast step allows interactions across different components during the model integration (Browne et al., 2019) and propagates the observational information to other components. In contrast, SCDA utilizes cross-component background error covariances to directly assimilate the observational information from one component into all components, treating the entire Earth system model as one unified system (Penny et al., 2019). Furthermore, similar to WCDA, SCDA also allows coupling in the forecast step to propagate the observations from one component to the other components (Yoshida and Kalnay, 2018). Several studies indicate that SCDA typically exhibits more pronounced improvements in assimilation performance relative to WCDA (Smith et al., 2015; Sluka et al., 2016). However, the application of SCDA poses substantial technical challenges, particularly in the establishment of effective cross-component background error covariances. Consequently, the majority of contemporary CDA systems still utilize the WCDA framework.

Recent research efforts have started to implement the CDA system to initialize DCPs, using a diverse range of DA techniques from simple to complex. The simplest method is nudging which adjusts the model states towards the observations or existing reanalysis (Hoke and Anthes, 1976; Zhang et al., 2020). Although the nudging method is time-saving and easy to implement, its application in CDA is restricted primarily due to the limited types of observations and the required interpolation of observations at every time step of model integration (He et al., 2017). Previous studies have developed advanced CDA systems using variational and filtering approaches, such as the three-dimensional variational data assimilation (3DVar) (Laloyaux et al., 2016; Yao et al., 2021), and ensemble-based techniques like the

ensemble Kalman filter (EnKF) (Zhang et al., 2007). The former generally utilizes the stationary background error covariance and assimilates observations sequentially (Lin et al., 2017). In contrast, the latter uses the flow-dependent forecast error covariance and recursively integrates observations into the model (Lei and Hacker, 2015). Several studies also show encouraging progress in constructing CDA systems using four-dimensional variational data assimilation (4DVar) method (Smith et al., 2015; Fowler and Lawless, 2016). The objective of 4DVar is to optimize four-dimensional model states and provide a compatible temporal trajectory that matches observational records across each assimilation window (Mochizuki et al., 2016). The 4DVar method is an advanced assimilation technique that exhibits superiority over other assimilation techniques like nudging and 3DVar in multiple aspects. Initial shocks that influence prediction skills can be significantly minimized by the 4DVar approach due to the dynamical consistency between the model and ICs (Sugiura et al., 2008). However, it is difficult to apply the 4DVar method for CDA systems in the fully coupled model because of the challenge in adjoint integration of the coupled model and its high computational cost in the analysis step. Finally, to capitalize on the strengths of both ensemble and variational techniques, recent studies focus on developing new hybrid data assimilation methods (Wang et al., 2010; Buehner et al., 2018). The hybrid approach utilizes an ensemble forecast to generate flow-dependent forecast error covariances and presents a way to perform 4DVar optimization without the need for tangent linear and adjoint models (Lorenc et al., 2015). However, most studies on CDA have focused on assimilating observations or reanalysis data of ocean, atmosphere and even sea ice. There have been relatively few instances of CDA studies assimilating land observations or reanalysis data.

In this study, we introduce the development of the 4DEnVar-based weakly coupled land data assimilation (WCLDA) system for the Energy Exascale Earth System Model version 2 (E3SMv2) (Golaz et al., 2022). The 4DEnVar method in this WCLDA system is the dimension-reduced projection 4DVar (DRP-4DVar; Wang et al., 2010) which utilizes the ensemble technique as an alternative to the adjoint technique for implementing 4DVar. In this WCLDA system, monthly mean anomalies of soil moisture and temperature from a global land reanalysis product are assimilated into the land component of a coupled climate model in the analysis step, and subsequently during the forecast step, the land reanalysis information incorporated into the ICs of the land component is propagated to the other components (e.g.,

删除了：Much work has been devoted to initializing climate models for practicable Earth system prediction, including uncoupled and coupled data assimilation (CDA) methods. Some modeling centers employ uncoupled initialization methods that directly utilize reanalysis data or stand-alone model states driven by observations as initial conditions (ICs) (Du et al., 2012; Prodhomme et al., 2016). However, ICs derived from uncoupled methods often exhibit poor consistency between model components (Balmaseda et al., 2009). Initializing a coupled model with data obtained from another model may result in initial shocks due to inconsistencies and eventually produce low prediction skills (Boer et al., 2016). A more effective initialization would involve performing a CDA with observations for each coupled model individually (Ardilouze et al., 2017). The CDA methods incorporate observations into one or several components of the coupled model through data assimilation techniques, with long-term assimilation cycles executed under the coupled modeling framework (He et al., 2020a). The CDA method outperforms the uncoupled method due to the constraint of the coupled model, leading to better consistency of the ICs with the coupled model (He et al., 2020b).

The CDA approaches for initializing coupled models are becoming increasingly prevalent, using a diverse range of data assimilation techniques. Most of these methods utilize simple nudging or nudging-based Incremental Analysis Update (IAU) approaches where analysis increments into a model integration are incorporated in a gradual manner

删除了：Some modeling centers have developed more advanced CDA systems using variational and filtering approaches, such as the three-dimensional variational data assimilation (3DVar) (Lin et al., 2017; Yao et al., 2021) and ensemble-based techniques like the ensemble Kalman filter (EnKF) (Santanello et al., 2016) or ensemble optimal

删除了：land

删除了：LCDA

删除了：LCDA

删除了：In this LCDA system, monthly mean soil moisture and temperature data from a global land reanalysis product are assimilated to

atmosphere and ocean) through the fully coupled model integration and influences the ICs of all components for the next assimilation window. The primary goal of the WCLDA system is intended to be a foundational resource for exploring predictability of the Earth system by the E3SM community, specifically focusing on understanding the sources of predictability provided by land versus ocean. This WCLDA system also provides the groundwork for future actionable predictions of Earth system variability using E3SM.

The objective of this paper is to introduce the implementation of the 4DEnVar-based WCLDA system for the land component of E3SMv2. In Sect. 2, we provide an overview of the E3SMv2 model, describe the 4DEnVar methodology in detail and outline the framework of the 4DEnVar-based WCLDA system. Preliminary evaluation of the WCLDA system is presented in Sect. 3. Finally, major conclusions are discussed in Sect. 4.

删除了：constrain the land fields of a coupled climate model with a one-month assimilation window.

删除了：LCDA

删除了：LCDA

设置了格式：字体颜色：红色

删除了：LCDA

删除了：LCDA

删除了：LCDA

2 Methods

2.1 Model Description

The model used in this study is a relatively new state-of-the-art Earth system model known as Energy Exascale Earth System Model version 2 (E3SMv2), supported by the U.S. Department of Energy (DOE) to improve actionable Earth system predictions and projections (Leung et al., 2020). The atmospheric component is the E3SM Atmosphere Model version 2 (EAMv2), which is built on the spectral-element atmospheric dynamical core with 72 vertical levels (Dennis et al., 2012; Taylor et al., 2020). At the standard resolution, EAMv2 is applied on a cubed sphere with a grid spacing of ~100 km for the dynamics. The ocean component is the Model for Prediction Across Scales-Ocean (MPAS-O), which applies the underlying spatial discretization to the primitive equations with 60 layers using a z-star vertical coordinate (Petersen et al., 2018; Reckinger et al., 2015). The sea ice component is MPAS-SI, which shares the same Voronoi mesh with MPAS-O, with mesh spacing varying between 60km in the mid-latitudes and 30 km at the equator and poles (Golaz et al., 2022). The land component is the E3SM Land Model version 2 (ELMv2), which is based on the Community Land Model version 4.5 (CLM4.5) (Oleson et al. 2013). Simulations are run in a satellite phenology mode with prescribed leaf area index, and the prescribed vegetation distribution has been updated for better consistency between land use and

changes in plant functional types described by Golaz et al. (2022). The river transport component is the Model for Scale Adaptive River Transport version 2 (MOSARTv2), which provides detailed representation of riverine hydrologic variables (Li et al., 2013). These five components exchange fluxes through the top-level coupling driver version 7 (CPL7) (Craig et al., 2012). Further details on the E3SMv2 model are described in Golaz et al. (2022).

2.2 Land Reanalysis Dataset

Monthly mean soil moisture and soil temperature data in total ten soil layers are produced by the Global Land Data Assimilation System (GLDAS; Rodell et al., 2004). The GLDAS products generate optimal fields of land surface states and fluxes in near-real time by forcing multiple offline land surface models with observation-based data fields. These reliable and high-resolution global land surface datasets from GLDAS are extensively utilized in weather and climate studies, hydrometeorological investigations and water cycle research (Chen et al., 2021; Zhang et al., 2018). The GLDAS datasets have been available globally at high spatial resolution since January 1979 and can be accessed through the Goddard Earth Science Data and Information Service Center. For more consistency with ELM, we utilize GLDAS data produced by CLM. Furthermore, we add the bias correction to GLDAS data before assimilation and conduct the anomaly assimilation for the WCLDA system in this study.

2.3 Data Assimilation Scheme

The 4DEnVar algorithm in this study is based on the DRP-4DVar technique, which is an efficient pathway for applying 4DVar through using the ensemble method rather than the adjoint technique (Wang et al., 2010). The DRP-4DVar method generates the optimal estimation in the sample space through aligning the observations with ensemble samples along the coupled model trajectory (Liu et al., 2011).

DRP-4DVar is an economical approach that minimizes the cost function of the standard 4DVar by using the ensemble technique instead of the adjoint technique (Wang et al., 2010). The B matrix is estimated using the pure ensemble covariance. The ensemble members originate from historical or ensemble forecasts. Considering the high computational cost of ensemble forecasts for the coupled model in our study, we utilize outputs from the Pre-industrial Control (PI-CTRL) experiment of E3SMv2 to

删除了：**Observational**

删除了：used in this study

删除了：↵

删除了：4Dvar

删除了：4Dvar

删除了：4Dvar

删除了：↵

设置了格式：字体颜色：文字 1

带格式的：缩进：首行缩进： 0.67 厘米

设置了格式：字体颜色：文字 1

generate ensemble members. The instantaneous state at the beginning of each month and the corresponding monthly mean state of this month from the 100-year balanced PI-CTRL simulation are used as the samples of initial condition (x_{ini}) and forecast samples (y_{ini}). The corresponding perturbation samples are calculated as $x'_{ini} = x_{ini} - \bar{x}$ and $y'_{ini} = y_{ini} - \bar{y}$, where $\bar{x}$ and $\bar{y}$ are the 100-year average values of x_{ini} and y_{ini} at the same month, respectively. Then, m pairs of perturbation samples ($x'_{1ini}, x'_{2ini}, x'_{3ini} \cdots, x'_{mini}$) and ($y'_{1ini}, y'_{2ini}, y'_{3ini} \cdots, y'_{mini}$) are selected at each DA analysis step according to the correlations between y'_{ini} and the observational innovation $y'_{obs} = y_{obs} - y_{ini}$ and the independence between y'_{ini} samples. In this study, $m = 30$. Then the estimation of the background error covariance matrix B is represented by the formula in Eq. (1), utilizing the selected x'_{ini} samples. To remove the spurious remote correlations in the B matrix, a localization approach is used (Wang et al., 2018).

$$\begin{cases} B = bb^T \\ b = \frac{1}{\sqrt{m-1}} \times (x'_1 - \bar{x'}, x'_2 - \bar{x'}, x'_3 - \bar{x'}, \cdots, x'_m - \bar{x'}) \\ \bar{x'} = \frac{1}{m}(x'_1 + x'_2 + x'_3 + \cdots + x'_m) \end{cases} \quad (1)$$

According to Wang et al. (2010), DRP-4DVar produces the analysis increment (x'_{ini}) by minimizing the 4DVar cost function in the incremental form (Courtier et al., 1994):

$$\begin{cases} J(x'_a) = \min_{x'} J(x') \\ J(x') = \frac{1}{2}(x')^T B^{-1} x' + \frac{1}{2}(\mathcal{Y}' - \mathcal{Y}'_{obs})^T (\mathcal{Y}' - \mathcal{Y}'_{obs}) \end{cases} \quad (2)$$

Here $x'_{ini} = x - x_{ini}$ represents the increment of model variables relative to the background; $\mathcal{Y}'_{obs} = r_{ini}^{-1} y'_{obs} = r_{ini}^{-1}(y_{obs} - y_{ini})$ denotes the weighted observational innovation for monthly mean soil moisture and temperature, and $R = r r_{ini}^T$ is the observational error covariance matrix that is usually diagonal; $\mathcal{Y}'_{ini} = r_{ini}^{-1} y'_{ini} = r_{ini}^{-1}(y - y_{ini})$ is the weighted prediction of innovation that is the projection of the increment (x'_{ini}) onto the observation space; the superscript T represents the transpose.

To simplify the calculation of the minimization, the increment of model state variables x'_{ini} and the corresponding weighted prediction of innovation $\mathcal{Y}'_{ini}$ are projected onto a dimension-reduced sample space through the following projection transformations:

$$\begin{cases} x' = P_x \alpha \\ \mathcal{Y}' = P_{\mathcal{Y}} \alpha \end{cases} \quad (3)$$

where α is the m-dimension column vector containing the weight coefficients ($\beta_{1ini}, \beta_{2ini}, \beta_{3ini} \cdots, \beta_{mini}$); $P_{\mathcal{Y}}$ and P_y denote the projection matrices that incorporate the initial condition perturbations and the

设置了格式 ... 3
设置了格式 ... 4
设置了格式 ... 5
设置了格式 ... 6
设置了格式 ... 7
设置了格式 ... 8
设置了格式 ... 9
设置了格式 ... 10
设置了格式 ... 11
设置了格式 ... 12
设置了格式 ... 13
设置了格式 ... 14
设置了格式 ... 15
设置了格式 ... 16
设置了格式: 字体颜色: 文字 1
设置了格式 ... 17
带格式的: 缩进: 首行缩进: 0.67 厘米, 无孤行控制
设置了格式: 字体颜色: 文字 1
设置了格式 ... 18
设置了格式 ... 19
设置了格式 ... 20
设置了格式 ... 21
设置了格式 ... 22
设置了格式 ... 23
设置了格式 ... 24
设置了格式 ... 25
设置了格式 ... 26
设置了格式 ... 27
设置了格式 ... 28
设置了格式 ... 29

corresponding monthly mean samples as follows:

$$\begin{cases} P_x = (x'_1, x'_2, x'_3, \cdots, x'_m) \\ P_{y'} = (y'_1, y'_2, y'_3, \cdots, y'_m)' \end{cases} \quad (4)$$

where $y'_i = \chi^{-1} y'_i$ $(i = 1, 2, \cdots, m)$. Then the original 4DVar cost function defined in Eq. (2) is transformed into the following new cost function and the analysis can be produced in the sample space by minimizing this new cost function:

$$\begin{cases} f(\alpha_a) = \min_{\alpha} f(\alpha) \\ f(\alpha) = \frac{1}{2}\alpha^T B_\alpha^{-1}\alpha + \frac{1}{2}(P_y\alpha - y'_{obs})^T(P_y\alpha - y'_{obs}) \\ x_a = x_b + x'_a = x_b + P_x\alpha_a \end{cases} \quad (5)$$

The solution to this minimization problem is formulated as:

$$\alpha_a = (B_\alpha^{-1} + P_y^T P_y)^{-1} P_y^T y'_{obs} \quad (6)$$

In this study, the DRP-4DVar-based CDA system is used to incorporate the land surface analysis data only. The optimal analysis for the land state variables (x_a^{lnd}) is obtained by adding the analysis increment (x'^{lnd}_a) to the background of land ICs (x_b^{lnd}), as expressed in Eq. (7):

$$x_a^{lnd} = x_b^{lnd} + x'^{lnd}_a = x_b^{lnd} + P_x(B_\alpha^{-1} + P_y^T P_y)^{-1} P_y^T y'_{obs} \quad (7)$$

In the analysis step, only the land state variables are updated to the optimal analysis (x_a^{lnd}). Subsequently, we proceed with a one-month free coupled integration of E3SMv2 model during the forecast step. This integration is initiated from the optimal land ICs (x_a^{lnd}) along with the background fields as the ICs of other components (e.g., atmosphere and ocean). Throughout this one-month free integration, the interactions among the model components indirectly enhance the background states of these components (e.g., atmosphere and ocean) for the next assimilation due to the more realistic land state variables. Moreover, this coupled integration also contributes to the good balance between the ICs of different components.

2.4 4DEnVar-based WCLDA System

The 4DEnVar-based WCLDA system is developed to assimilate the monthly mean soil moisture and temperature data from the GLDAS analysis dataset into the land component of E3SMv2 using the DRP-4DVar method. Two sets of numerical experiments are conducted to evaluate the performance of land data assimilation in the WCLDA system. The control simulation (CTRL) is a 36-year freely coupled

设置了格式 ... 30
设置了格式 ... 31
设置了格式 ... 32
设置了格式 ... 33
设置了格式 ... 34
设置了格式 ... 35
设置了格式 ... 36
设置了格式 ... 37
设置了格式: 字体颜色: 文字 1
设置了格式 ... 38
设置了格式 ... 39

删除了: Following Wang et al. (2010), the original 4DVar can be implemented to produce the optimal analysis in the sample space by minimizing a new cost function:
= += +
(1)
= (2)
= α + (α−) (3)
The optimal solution to the aforementioned minimization problem is formulated as:
= (4)
Here, , , and represent the optimal analysis, background, and analysis increment, respectively; is the projection matrix comprised of initial perturbation samples; α is the weight coefficients; the superscript T represents the transpose; B denotes the background error covariance matrix; is the projection matrix consisting of observational perturbation samples; represents the weighted observational innovation.

删除了: LCDA

删除了: LCDA…CLDA system is developed to assimilate the full-field …onthly mean soil moisture and temperature data from the GLDAS analysis dataset into the land component of E3SMv2 using the DRP-4DVar method. Two sets of numerical experiments are conducted to evaluate the performance of land data assimilation in the LCDA ... 40

integration driven by observed external forcing from 1980 to 2016. The freely coupled simulation implies that the various components of our Earth system model, namely the atmosphere, land, river, ocean, and sea ice, are interacting dynamically without any restraints. The observed external forcing mainly acts on the atmospheric component and then influences other components (e.g., land surface, ocean, and sea ice) through the atmosphere. CTRL provides the benchmark for assessing the performance of the WCLDA system. The assimilation experiment (Assim) is conducted from 1980 to 2016 based on the WCLDA system in which the GLDAS data are assimilated into the land state variables from the first to the tenth layer with a one-month assimilation window under the coupled modeling framework. The effectiveness of the WCLDA system is evaluated through the comparison between Assim and CTRL. In both Assim and CTRL, the transient-historical external forcings are prescribed following the CMIP6 protocol (Eyring et al., 2016). In contrast to decadal timescales, data signals with temporal resolutions shorter than one month can potentially introduce undesirable noise, adversely affecting the DCPs upon assimilation into the ICs. Moreover, it is also very difficult to assimilate complex actual observations in the initialization for DCPs that needs long-term DA cycles due to the very high computational cost. Therefore, similar to most existing initialization approaches for DCPs that assimilate reanalysis data, this study initialize the DCPs by assimilating monthly mean GLDAS data within the one-month assimilation window.

The flowchart of the 4DEnVar-based WCLDA system is illustrated in Figure 1. The DRP-4DVar method incorporates three inputs: model background, observational innovation and 30 perturbation samples. First, the E3SMv2 model is executed for one month, during which state variables such as model background (x_b), observational operator (H) and observational background (y_b) are stored. The model background (x_b) denotes monthly initial states before assimilation, and the observational operator (H) represents a one-month integration by the coupled model to generate monthly mean model outputs (y_b). Second, upon completion of the one-month coupled run, the observational innovation ($\boldsymbol{y}'_{obs}$) is determined by calculating the differences in soil moisture and temperature between the monthly mean GLDAS data (y_{obs}) and model outputs (y_b). From the 100-year sample database of the E3SMv2 PI-CTRL simulation, 30 monthly mean perturbation samples ($\boldsymbol{y}'$) are chosen according to the highest absolute correlation with the observational innovation. The corresponding 30 monthly IC samples (x') are also obtained. Finally, the analysis increment is generated in the sample space and the optimal analysis (x_a) is calculated using

设置了格式：字体颜色：文字 1

删除了：LCDA

删除了：LCDA

删除了：LCDA

设置了格式：字体颜色：文字 1

设置了格式：字体颜色：红色

删除了：LCDA

删除了：Pre-industrial Control (

删除了：)

the DRP-4DVar algorithm. To alleviate the spurious correlations, a localization scheme is implemented in the 4DEnVar-based WCLDA system (Wang et al., 2018).

The schematic diagram in Figure 2 outlines the assimilation process of the 4DEnVar-based WCLDA system in E3SMv2. The incorporation of GLDAS data into the E3SMv2 model consists of the analysis step and the forecast step. In the analysis step, the differences between monthly mean GLDAS data and model outputs are calculated, and are then utilized to produce the optimal assimilation analysis at the beginning of a one-month assimilation window. Subsequent to this, in the forecast step, this optimal assimilation analysis is used to as the land surface ICs combined with background ICs for other components to conduct one-month forecast using E3SMv2 model. This forecast generates the backgrounds of all components for the next assimilation. As a result, the forecasted backgrounds for all components are influenced by the observed land information incorporated into the ICs of land surface component. In general, when the coupled model is used in the forecast step but the optimal assimilation analysis is updated separately for the respective component, the assimilation approach is identified as WCDA (Penny et al., 2019; Zhang et al., 2020). The detailed assimilation process mainly consists of three steps within each one-month assimilation window: 1) the E3SMv2 model is initially executed for one month to generate the simulated monthly mean soil moisture and temperature (y_b^{lnd}); 2) the observational innovation (y'_{obs}) is obtained through subtracting model simulation (y_b^{lnd}) from the monthly mean observation (y_{obs}^{lnd}). This innovation is then applied to formulate the optimal assimilation analysis of land surface (x_a^{lnd}) at the beginning of the assimilation window through the DRP-4DVar method; 3) the E3SMv2 model is rewound to the start of the month and the second one-month model run is executed using the optimal ICs (x_a) to generate the background for the next assimilation cycle. Due to land-atmosphere-ocean interactions during the one-month free coupled integration, the observed land information can potentially benefit other components (e.g., atmosphere and ocean) in the coupled modeling framework (Li et al., 2021; Shi et al., 2022). To assimilate the monthly mean GLDAS product, the fully coupled integration by E3SMv2 model is performed twice within each one-month assimilation window: first to generate the observational innovation by computing the differences between GLDAS data and model outputs for analysis, and second to forecast the backgrounds of all components for the next assimilation. When the fully coupled model is executed for the second one-month run, the observed

删除了：LCDA

删除了：LCDA

设置了格式： 字体颜色：文字 1

设置了格式： 字体颜色：文字 1

设置了格式： 字体颜色：文字 1

设置了格式： 字体颜色：文字 1

设置了格式： 字体颜色：文字 1

设置了格式： 字体颜色：文字 1

设置了格式： 字体颜色：文字 1

设置了格式： 字体颜色：文字 1

删除了：multi-component interactions

设置了格式： 字体颜色：文字 1

设置了格式： 字体颜色：文字 1

设置了格式： 字体颜色：文字 1

设置了格式： 字体颜色：文字 1

设置了格式： 字体颜色：文字 1

land information is transferred into the other components through multi-component interactions. Similarly, to assimilate the monthly GRACE-based TWS observations, previous studies employed the "two-step" scheme in which the land model integration is performed twice within the same month (Houborg et al., 2012; Girotto et al., 2016).

2.5 Evaluation Metrics

The reduction rate of the cost function is a significant metric for verifying the effectiveness of the WCLDA system and evaluating the extent of observational information assimilated by the coupled model, which is formulated as:

$$\begin{cases} \frac{J_1 - J_0}{J_0} \times 100\% \\ J_0 = \frac{1}{2}(y_{obs} - y_b)^T R^{-1}(y_{obs} - y_b) \\ J_1 = \frac{1}{2}(y_{obs} - y_a)^T R^{-1}(y_{obs} - y_a) \end{cases} \quad (8)$$

where J_0 and J_1 denotes the observational cost function before and after assimilation respectively, y_{obs} represents the GLDAS data, y_a denotes the monthly mean analyses, y_b is the observation-space background, and R is defined as the observation error covariance matrix. Negative value for this metric indicates that observational information has been correctly incorporated into the model variables.

Following Yin et al. (2014), the assimilation efficiency (AE) index is defined to evaluate the efficiency of the WCLDA system as follows:

$$AE = \frac{RMSE_{Assim}}{RMSE_{CTRL}} - 1 \quad (9)$$

In this equation, $RMSE_{Assim}$ is the root mean square error (RMSE) between Assim and the reference data, while $RMSE_{CTRL}$ represents the RMSE between CTRL and the reference data. Negative (positive) AE value indicates improvements (degradations) by the assimilation. In the following sections, we continue to use the GLDAS data as the reference dataset to verify the correctness of the WCLDA system.

3 Results

3.1 Evaluation of the cost function

Figure 3 displays the time series of the monthly reduction rate of the cost function in the 4DEnVar-based WCLDA system. In the first month, the reduction rate reaches approximately 26.06% in Assim.

删除了：LCDA
删除了：× 100%
删除了：
删除了：5
删除了：LCDA
删除了：6
删除了： GLDAS data
删除了：GLDAS data
删除了：LCDA
删除了：LCDA
删除了：28.8

Over the subsequent months, Assim maintains the average reduction rate of 7.73% throughout the entire period. Furthermore, negative reduction rates are observed in 98.65% of the total months, indicating the effectiveness of the WCLDA system. These results suggest that the WCLDA system is correctly implemented, with the observational data successfully assimilated into the coupled model.

3.2 Evaluation of the AE index

The spatial pattern of the AE index for soil moisture at different depths is depicted in Figure 4. The AE value exhibits negative signal in most areas from total ten soil layers, suggesting the reduction in RMSE for soil moisture after assimilation. Significant improvements appear over North America, South America, southern Africa, Europe, and Asia. However, assimilation performance is degraded in the northern part of Russia and northern Africa. This is consistent with the findings in other studies that assimilation updates in northern Russia are limited due to the complexities of accurately representing frozen ground and snow processes in high latitudes (Edwards et al., 2007; Ireson et al., 2013). The surface soil moisture is highly susceptible to atmospheric conditions, subsequently affecting the assimilation performance. Furthermore, some degradations found in the deep layers could be attributed to the substantial influence of various terrestrial factors, such as subsurface runoff and interactions with groundwater, similar to the findings in previous studies (Liu and Mishra, 2017; Zeng and Decker, 2009).

Figure 5 shows the spatial distribution of the AE index for soil temperature from surface to deep layers. Most grid cells from total ten soil layers are dominated by negative AE signals, indicating improved performance for soil temperature after assimilation. Moreover, the spatial patterns across different soil layers are highly consistent with each other and exhibit similar magnitudes in most areas. Notable improvements are observed in central Europe, South America, eastern Russia, and large parts of Eurasia and North America. In contrast, slight degradations appear over Southeast Asia and along the northern fringes of Africa. This may be partly related to model uncertainties and possible atmospheric noise, as shown by many past studies (Kwon et al., 2016; Lin et al., 2020).

We further perform our analysis to the spatial pattern of the AE index for surface soil moisture and land surface temperature between MODIS data and model simulations (Figure A1) in the Appendix. For surface soil moisture, the comparison with MODIS data suggests that the majority of global regions

删除了：8.5

删除了：96

删除了：LCDA

删除了：LCDA

删除了： the second to the eighth layer

删除了：Northern Africa

删除了：Northern

删除了：The largest improvement in these soil layers is observed in the northern part of the Eurasian continent.

删除了：South America and monsoon regions (e.g., East Asia and India).

删除了：monsoon regions

删除了：the dominant impact of monsoon circulations (Timouk et al., 2009; Brocca et al., 2017). The first soil layer, which is highly susceptible to atmospheric forcing, also shows degradation in large areas.

删除了：are

删除了：, especially the ninth and tenth layers. This may be linked to

删除了： the quality of assimilation data and other terrestrial factors, as noted in previous studies (Liu and Mishra, 2017; Zeng and Decker, 2009).

删除了：the first to the ninth layer

删除了：Eastern Russia, Europe, North America, Australia, and large parts of Eurasia.

删除了：Northwestern Africa, Southern South America and Saudi Arabia.

删除了：assimilation

删除了：

exhibit reduced RMSE after assimilation. The reduction of RMSE is pronounced in central North America, South America, southern Africa, Australia, and Europe. However, in high-latitude areas, significant degradations are observed in northern Russia, which may be possibly related to model deficiencies in simulating the complex frozen ground and snow processes. Regarding land surface temperature, improved performances are evident over South America, Australia, southern Africa, and parts of Eurasia when compared to MODIS data. In contrast, some degradations appear over parts of North America and central Asia, which still require further improvement.

3.3 Evaluation of the correlation

Figure 6 displays the spatial patterns of the differences in temporal correlations for soil moisture between Assim and CTRL with observations across different soil layers. The majority of global regions in Assim exhibit higher correlations from the first to the tenth layer compared with CTRL, suggesting the overall good performance of the WCLDA system. Enhanced correlations in deep soil layers are more pronounced than in shallow layers, which may be attributed to the longer memory of soil processes in the deeper layers (Wang et al., 2010). Improved correlations appear over North America, central Europe, Asia, and parts of Africa. However, some scattered areas show slight degradations, such as northern South America, central Africa, and eastern Russia. Overall, Assim outperforms CTRL with higher correlation (Figure 6) and lower RMSE (Figure 4) in many regions, such as Europe, North America, southern South America, and South Asia.

The correlation differences in soil temperature between Assim and CTRL from surface to deep layers are shown in Figure 7. Assim yields improved correlations from the first to the tenth layer across the majority of global regions. Furthermore, similar spatial patterns and magnitudes are observed in the performance of different soil layers, implying the significant heat transfer from the surface to deep zone that constrains soil temperature across the soil column. Notable improvements are located over South America, central Africa, Australia, central Europe, and East Asia. Nevertheless, some degradations appear over North America, western Europe, and Northeast China. Assim shows superior performance over CTRL for soil temperature with higher correlation (Figure 7) and lower RMSE (Figure 5) in many regions, including South America, central Europe, Australia, and central Africa.

删除了： Some locations with degradation are also noted in the tenth layer, which still requires further improvement.

删除了： A

删除了： LCDA

删除了： prominent

删除了： Northern Africa, North America, Eurasia, and Australia.

删除了： Central Africa, and Eastern Russia.

删除了： Western Russia, Northern Africa, North America, and Central Eurasia.

删除了： ninth

删除了： global domain, with the exception of the northern region of the Eurasian continent.

删除了： except for the tenth layer,

删除了： North America, Northern Africa, Australia, and Southern Eurasia.

删除了： Central Africa, Eastern Russia, and part of South China. Obvious degradations are also found in the tenth layer. The diminished performance may come from uncertainties in the assimilation data and imbalances between land variables during data assimilation, as supported by the findings of other studies (Park et al., 2018; Zhang et al., 2014).

删除了： Southern Eurasia, Australia, and North America.

3.4 RMSE and bias of the global mean soil moisture and temperature

The vertical distributions of RMSE differences between Assim and CTRL for soil moisture and temperature are evaluated in Figure 8. Assim shows noticeable improvements with reduced RMSE for both soil moisture and temperature from total ten soil layers compared with CTRL. For soil moisture, the reduction of RMSE increases with depth from the upper to deep levels, reaching its maximum at the tenth layer. This could be attributed to the longer soil memory in deep layers than shallow layers. For soil temperature, the reduction of RMSE exhibits similar magnitude from the surface to deep soil layers, which may be explained by the significant heat transfer across different soil layers in regulating soil temperature throughout the soil column.

Figure 9 shows the time evolutions of the vertically averaged global mean soil moisture and temperature bias and RMSE differences. For soil moisture bias (Figure 9a), CTRL exhibits dry biases during the first twenty years and wet biases afterwards. In contrast, Assim shows smaller biases during both periods by reducing the dry bias prior to ~2000 and the wet bias thereafter. Assim also exhibits reduced RMSE (Figure 9b) for soil moisture throughout the entire 37-year period. For soil temperature bias (Figure 9c), CTRL and Assim display comparable performances, possibly due to the small magnitude of model deviation in soil temperature. The RMSE differences (Figure 9d) suggest that Assim decreases the RMSE for soil temperature in the majority of months, with 74.10% of the total months in Assim exhibiting lower RMSE than CTRL. In summary, the superior performance for both soil moisture and temperature in Assim demonstrates that land observational information has been effectively incorporated into the model variables through the WCLDA system.

Noticeably, the simulated soil temperature and soil moisture display similar long-term trends, with cold and dry biases before ~2000 and warm and wet biases afterwards. The soil temperature biases may be related to the global surface air temperature simulated in E3SMv2, which is notably too cold compared to the observed record during the 1970s and 1980s while the model warms up quickly after ~year 2000 (see Figure 23 of Golaz et al., 2022). The global surface air temperature biases in E3SMv1 and v2 during the past decades have been attributed to the strong aerosol forcing in the model (Golaz et al., 2019; 2022). As the global mean precipitation scales with the surface temperature at ~2% per degree (Allen and Ingram,

删除了：

删除了： at all vertical levels

删除了： middle

删除了： eighth

删除了：

删除了： However, this value then decreases as the depth extends further into the tenth layer. This decrease is likely due to the overestimation of observation errors in deep soil layers.

删除了： across shallow layers

删除了： process within the soil. From the middle to deep levels, this reduction initially increases with depth, peaking at the eighth layer, and then gradually decreases. In the ninth and tenth layers, there is potential for further improvement in assimilation performance.

删除了： in most months,

删除了： 91.7

删除了： LCDA

2002), model biases in surface temperature are reflected in biases in precipitation and hence soil moisture, resulting in similar long-term trends between soil temperature and soil moisture biases in the simulations.

3.5 2012 U.S. Midwest Drought

To further evaluate the performance of the WCLDA system, we preliminarily investigate the impact of land data assimilation on simulating the temporal evolution of the U.S. Midwest drought in 2012. Time series of soil moisture percentiles over the Midwest (36°-50°N, 102°-88°W) demonstrate significant improvements by Assim in reproducing the time evolution of agricultural drought in 2012 compared with CTRL (Figure 10). From the observation based on ERA-Interim data, the agricultural drought starts in August 2011, follows by a brief relief in early spring of 2012, peaks in September 2012, and recovers by January 2013. The drought develops rapidly between May and July 2012 over a wide-spread area including the central and midwestern U.S. This flash drought caused significant agricultural damages and economic losses.

The free running CTRL experiment fails to simulate the temporal evolution of the 2012 Midwest drought, with a correlation coefficient between CTRL and observation of only 0.27. The onset and peak of the drought are remarkably well captured by Assim, although the drought recovery occurs two months later than observed. The correlation coefficient of the Assim time series with observation is 0.56, which is statistically significant at the 95% confidence level. Our results highlight the importance of land surface states for drought lifecycle, with the potential to improve future drought predictions through the implementation of the WCLDA system.

We further conduct the comparative analysis to investigate the impacts of full-field versus anomaly land assimilation on simulating the temporal evolutions of soil moisture (Figure A2) and precipitation (Figure A3) variability during the 2012 Midwest drought in the Appendix. Full-field assimilation utilizes actual observed values for model initialization, whereas anomaly assimilation employs only observed anomalies. The full-field assimilation exhibits a correlation coefficient of 0.61 with observed soil moisture (Figure A2), higher than that of anomaly assimilation (0.56). Furthermore, it is noteworthy that the full-field assimilation significantly outperforms the anomaly assimilation in capturing the precipitation anomaly variability (Figure A3). More specifically, the full-field assimilation can reproduce the positive

删除了： LCDA

删除了： one month earlier than observed.

删除了： 0.61

删除了：

删除了： LCDA

precipitation anomaly from February 2012 to April 2012 and the dry anomaly from May 2012 to October 2012. The correlation coefficient of the full-field assimilation with observed precipitation is 0.40, much higher than a low correlation of -0.03 from anomaly assimilation. These results underscore the enhanced capability of full-field assimilation to reproduce both soil moisture and precipitation variability more accurately than anomaly assimilation during the 2012 Midwest drought, suggesting its potential for more reliable drought-related simulations.

4 Conclusions

In this study, we developed the 4DEnVar-based WCLDA system for the E3SMv2 model and evaluated the performance of this WCLDA system. The DRP-4DVar method was employed for implementing 4DVar using the ensemble method rather than the adjoint technique. Special attention is paid to directly assimilating monthly mean land reanalysis data in this system without interpolating to every time step. Within each one-month assimilation window, we assimilate observed land information into the coupled model without breaking the land-atmosphere interaction, which is important for the WCLDA system to be used to understand the potential sources of predictability provided by land.

The WCLDA system is conducted from 1980 to 2016, and its performance is evaluated using multiple metrics, including the cost function, AE index, correlation, RMSE and bias. Compared with CTRL, the cost function is reduced by Assim in most months, suggesting that observational data has been effectively incorporated into the model. In terms of both soil moisture and temperature, Assim outperforms CTRL with lower RMSE and higher temporal correlation in many regions, especially in South America, central Africa, Australia, and large parts of Eurasia. However, some degradations are observed in the deep layers, which requires future research to better characterize observation errors in these deep zones. For soil moisture bias, Assim further decreases the dry bias during the first twenty years and the wet bias thereafter. It is noteworthy that the subseasonal-to-seasonal time evolution of soil moisture percentiles during the 2012 U.S. Midwest drought can be quite well captured in Assim, underscoring the significant role of land surface states in drought propagation.

Our current WCLDA system has some limitations and future improvements in the WCLDA system will depend on integrating actual observations (e.g., satellite and station data). Specifically, one significant

删除了： compare the time series of observed and simulated precipitation anomaly over the Midwest during the 2012 U.S. Midwest drought (Figure 11). As a free running simulation, the precipitation in CTRL is not expected to reproduce the overall dry anomaly in observation. It is noteworthy that the magnitude of the precipitation anomaly is remarkably well captured by Assim. More specifically, Assim can reproduce the positive precipitation anomaly from February 2012 to April 2012 and the dry anomaly from May 2012 to October 2012. The correlation coefficient of the Assim time series with observation is 0.40, much higher than that of CTRL (-0.21). The dramatic increase in the correspondence in precipitation between Assim and observation strongly suggests that the effects of land data assimilation can transmit to the atmosphere through land-atmosphere interactions in the LCDA system, which may improve precipitation simulation. Improvements in the atmosphere states through land data assimilation highlight the important role of the land surface in drought development.

删除了： LCDA

删除了： the

删除了： LCDA

删除了： ,

删除了： as needed in the nudging method.

删除了： LCDA

删除了： LCDA

删除了： North America, Northern Africa, Australia, and large parts of Eurasia.

删除了： The dramatic increase in the temporal correlations for precipitation anomaly in Assim also demonstrates that the impacts of land data assimilation could potentially contribute to the improvement in the atmospheric states through land-atmosphere interactions, highlighting the importance of the land surface in drought development.

删除了： F

删除了： LCDA

删除了： the use of more observations

limitation in this WCLDA system is the lack of the observation operator, making it challenging to assimilate actual observations at this stage. The observation operator is crucial in providing the linkage between the model variables and actual observations, considering their diverse spatial and temporal resolutions. Further exploration will focus on developing observation operators suitable for assimilating various satellite data, such as the AMSR-E and GRACE data. It is possible that the influence of the WCLDA system on atmospheric process may be restricted in specific domains due to the model characterizations, particularly in the representation of land-atmosphere interactions (Zhou et al., 2023). For example, in humid regions where the evaporation process is predominantly energy-limited, the assimilation of soil moisture tends to exert limited influence. Instead, the assimilation of soil temperature may yield substantial improvements. This underscores the importance of the unique characteristics and constraints presented by complicated regional conditions in the application of assimilation processes. To this end, the application of the WCLDA system would motivate future work to better understand the roles of the land surface in climate variability and provide a foundational resource for future predictability studies by the E3SM community.

Code and data availability. The E3SMv2 source codes used in this study can be accessed on Zenodo at https://zenodo.org/record/8194050. The GLDAS monthly soil moisture and soil temperature data can be downloaded from the website https://disc.gsfc.nasa.gov/datasets?keywords=GLDAS%20monthly&page=1. The GPCP monthly precipitation data are available online (https://psl.noaa.gov/data/gridded/data.gpcp.html). The ERA-Interim monthly soil moisture data are available at https://apps.ecmwf.int/archive-catalogue/?levtype=sfc&type=an&class=ei&stream=moda&expver=1. The model data used in this study can be found on Zenodo at https://zenodo.org/record/8148737.

Author contributions. LRL initiated this study. PS and LRL designed the experiments. BW provided advice on the data assimilation technique and KZ and SZ provided assistance with the E3SM model. PS developed the data assimilation code and performed the simulations. PS and LRL analyzed and interpreted the data. PS and LRL wrote the paper. BW, KZ, SMH, and SZ contributed to the revision.

删除了： and improving the quality of the ensemble covariance.

删除了： assimilation performance is restricted in specific domains due to biased atmospheric and oceanic forcing from the coupled model. Hence the continual integration of atmospheric and oceanic assimilations into the LCDA system could be an important way to further enhance its performance, particularly in regions where the land is primarily influenced by other components. Given the independence of the LCDA system from the coupled model, future exploration will focus on its implementation in other model components (e.g., atmosphere, ocean, and sea ice) or different climate models.

删除了： LCDA

Competing interests. The authors declare no competing interests.

Acknowledgements. This research was supported by the Office of Science, Department of Energy Biological and Environmental Research as part of the Regional and Global Model Analysis program area. Pacific Northwest National Laboratory is operated by Battelle Memorial Institute for the U.S. Department of Energy under contract DE-AC05-76RL01830.

824 **References**

825 Allen, M. R., and Ingram, W. J.: Constraints on future changes in climate and the hydrologic cycle, Nature,
826 419, 224–232, https://doi.org/10.1038/nature01092, 2002.

827 Ardilouze, C., Batté, L., Bunzel, F., Decremer, D., Déqué, M., Doblas-Reyes, F. J., Douville, H., Fereday,
828 D., Guemas, V., MacLachlan, C. and Müller, W.: Multi-model assessment of the impact of soil
829 moisture initialization on mid-latitude summer predictability, Climate Dynamics, 49, 3959–3974,
830 https://doi.org/10.1007/s00382-017-3555-7, 2017.

831 Balmaseda, M. A., Alves, O. J., Arribas, A., Awaji, T., Behringer, D. W., Ferry, N., Fujii, Y., Lee, T.,
832 Rienecker, M., Rosati, T. and Stammer, D.: Ocean initialization for seasonal forecasts,
833 Oceanography, 22(3), 154–159, https://doi.org/10.5670/oceanog.2009.73, 2009.

834 Bellucci, A., Gualdi, S., Masina, S., Storto, A., Scoccimarro, E., Cagnazzo, C., Fogli, P., Manzini, E., and
835 Navarra, A.: Decadal climate predictions with a coupled OAGCM initialized with oceanic
836 reanalyses, Climate Dynamics, 40, 1483–1497, https://doi.org/10.1007/s00382-012-1468-z, 2013.

837 Boer, G. J., Smith, D. M., Cassou, C., Doblas-Reyes, F., Danabasoglu, G., Kirtman, B., Kushnir, Y.,
838 Kimoto, M., Meehl, G. A., Msadek, R. and Mueller, W. A.: The decadal climate prediction project
839 (DCPP) contribution to CMIP6, Geoscientific Model Development, 9(10), 3751–3777,
840 https://doi.org/10.5194/gmd-9-3751-2016, 2016.

841 Browne, P. A., De Rosnay, P., Zuo, H., Bennett, A., and Dawson, A.: Weakly coupled ocean-atmosphere
842 data assimilation in the ECMWF NWP system, Remote Sensing, 11(3), 234,
843 https://doi.org/10.3390/rs11030234, 2019.

844 Buehner, M., Du, P., and Bédard, J.: A new approach for estimating the observation impact in ensemble–
845 variational data assimilation, Monthly Weather Review, 146(2), 447-465,
846 https://doi.org/10.1175/MWR-D-17-0252.1, 2018.

847 Chen, Z., Zeng, Y., Shen, G., Xiao, C., Xu, L., and Chen, N. C.: Spatiotemporal characteristics and
848 estimates of extreme precipitation in the Yangtze River Basin using GLDAS data, International
849 Journal of Climatology, 41, 1812–1830, https://doi.org/10.1002/joc.6813, 2021.

850 Collins, M. and Allen, M. R.: Assessing the relatives roles of initial and boundary conditions in
851 interannual to decadal climate predictability, Journal of Climate, 15, 3104–3109,

删除了： Bloom, S. C., Takacs, L. L., Da Silva, A. M., and Ledvina, D.: Data assimilation using incremental analysis updates, Monthly Weather Review, 124(6), 1256–1271, https://doi.org/10.1175/1520-0493(1996)124<1256:DAUIAU>2.0.CO;2, 1996.

删除了： Brocca, L., Crow, W. T., Ciabatta, L., Massari, C., De Rosnay, P., Enenkel, M., Hahn, S., Amarnath, G., Camici, S., Tarpanelli, A. and Wagner, W.: A review of the applications of ASCAT soil moisture products, IEEE Journal of Selected Topics in Applied Earth Observations and Remote Sensing, 10(5), 2285–2306, https://doi.org/10.1109/JSTARS.2017.2651140, 2017.

https://doi.org/10.1175/1520-0442(2002)015<3104:ATRROI> 2.0.CO;2, 2002.

Conil, S., Douville, H., and Tyteca, S.: The relative influence of soil moisture and SST in climate predictability explored within ensembles of AMIP type experiments, Climate Dynamics, 28, 125–145, https://doi.org/10.1007/s00382-006-0172-2, 2007.

Courtier, P., Thépaut, J. M., and Hollingsworth, A.: A strategy for operational implementation of 4D-Var, using an incremental approach, Quarterly Journal of the Royal Meteorological Society, 120, 1367–1387, https://doi.org/10.1002/qj.49712051912, 1994.

Craig, A. P., Vertenstein, M., and Jacob, R.: A new flexible coupler for Earth system modeling developed for CCSM4 and CESM1, International Journal of High Performance Computing Applications, 26(1), 31–42, https://doi.org/10.1177/1094342011428141, 2012.

Dee, D. P., Balmaseda, M., Balsamo, G., Engelen, R., Simmons, A. J., and Thépaut, J. N.: Toward a consistent reanalysis of the climate system, Bulletin of the American Meteorological Society, 95(8), 1235-1248, https://doi.org/10.1175/BAMS-D-13-00043.1, 2014.

Dennis, J. M., Edwards, J., Loy, R., Jacob, R., Mirin, A. A., Craig, A. P., and Vertenstein, M.: An application-level parallel I/O library for Earth system models, International Journal of High Performance Computing Applications, 26(1), 43–53, https://doi.org/10.1177/1094342011428143, 2012.

Du, H., Doblas-Reyes, F. J., García-Serrano, J., Guemas, V., Soufflet, Y., and Wouters, B.: Sensitivity of decadal predictions to the initial atmospheric and oceanic perturbations, Climate Dynamics, 39(7), 2013–2023, https://doi.org/10.1007/s00382-011-1285-9, 2012.

Edwards, A. C., Scalenghe, R., and Freppaz, M.: Changes in the seasonal snow cover of alpine regions and its effect on soil processes: a review, Quaternary International, 162, 172–181, https://doi.org/10.1016/j.quaint.2006.10.027, 2007.

Eyring, V., Bony, S., Meehl, G. A., Senior, C. A., Stevens, B., Stouffer, R. J., and Taylor, K. E.: Overview of the Coupled Model Intercomparison Project Phase 6 (CMIP6) experimental design and organization, Geoscientific Model Development, 9, 1937–1958, https://doi.org/10.5194/gmd-9-1937-2016, 2016.

Fowler, A. M., and Lawless, A. S.: An idealized study of coupled atmosphere–ocean 4D-Var in the

presence of model error, Monthly Weather Review, 144(10), 4007–4030, https://doi.org/10.1175/MWR-D-15-0420.1, 2016.

Ireson, A. M., Van Der Kamp, G., Ferguson, G., Nachshon, U., and Wheater, H. S.: Hydrogeological processes in seasonally frozen northern latitudes: understanding, gaps and challenges, Hydrogeology Journal, https://doi.org/10.1007/s10040-012-0916-5, 2013.

Girotto, M., De Lannoy, G. J., Reichle, R. H., and Rodell, M.: Assimilation of gridded terrestrial water storage observations from GRACE into a land surface model, Water Resources Research, 52(5), 4164–4183, https://doi.org/10.1002/2015WR018417, 2016.

Golaz, J. C., Caldwell, P. M., Van Roekel, L. P., Petersen, M. R., Tang, Q., Wolfe, J. D., Abeshu, G., Anantharaj, V., Asay-Davis, X. S., Bader, D. C., Baldwin, S. A., Bisht, G., Bogenschutz, P. A., Branstetter, M., Brunke, M. A., Brus, S. R., Burrows, S. M., Cameron-Smith, P. J., Donahue, A. S., Deakin, M., Easter, R. C., Evans, K. J., Feng, Y., Flanner, M., Foucar, J. G., Fyke, J. G., Griffin, B. M., Hannay, C., Harrop, B. E., Hoffman, M. J., Hunke, E. C., Jacob, R. L., Jacobsen, D. W., Jeffery, N., Jones, P. W., Keen, N. D., Klein, S. A., Larson, V. E., Leung, L. R., Li, H. Y., Lin, W., Lipscomb, W. H., Ma, P. L., Mahajan, S., Maltrud, M. E., Mametjanov, A., McClean, J. L., McCoy, R. B., Neale, R. B., Price, S. F., Qian, Y., Rasch, P. J., Reeves Eyre, J. E. J., Riley, W. J., Ringler, T. D., Roberts, A. F., Roesler, E. L., Salinger, A. G., Shaheen, Z., Shi, X., Singh, B., Tang, J., Taylor, M. A., Thornton, P. E., Turner, A. K., Veneziani, M., Wan, H., Wang, H., Wang, S., Williams, D. N., Wolfram, P. J., Worley, P. H., Xie, S., Yang, Y., Yoon, J.-H., Zelinka, M. D., Zender, C. S., Zeng, X., Zhang, C., Zhang, K., Zhang, Y., Zheng, X., Zhou, T., and Zhu, Q.: The DOE E3SM Coupled Model Version 1: Overview and Evaluation at Standard Resolution, Journal of Advances in Modeling Earth Systems, 11, 2089–2129, https://doi.org/https://doi.org/10.1029/2018MS001603, 2019.

Golaz, J. C., Van Roekel, L. P., Zheng, X., Roberts, A. F., Wolfe, J. D., Lin, W. Y., Bradley, A. M., Tang, Q., Maltrud, M. E., Forsyth, R. M., Zhang, C. Z., Zhou, T., Zhang, K., Zender, C. S., Wu, M. X., Wang, H. L., Turner, A. K., Singh, B., Richter, J. H., Qin, Y., Petersen, M. R., Mametjanov, A., Ma, P., Larson, V. E., Krishna, J., Keen, N. D., Jeffery, N., Hunke, E. C., Hannah, W. M., Guba, O., Griffin, B. M., Feng, Y., Engwirda, D., Vittorio, A. V., Cheng, D., Conlon, L. M., Chen, C., Brunke, M. A., Bisht, G., Benedict, J. J., Asay-Davis, X. S., Zhang, Y. Y., Zhang, M., Zeng, X. B., Xie, S.

C., Wolfram, P. J., Vo, T., Veneziani, M., Tesfa, T. K., Sreepathi, S., Salinger, A. G., Jack Reeves Eyre, J. E., Prather, M. J., Mahajan, S., Li, Q., Jones, P. W., Jacob, R. L., Huebler, G. W., Huang, X. L., Hillman, B. R., Harrop, B. E., Foucar, J. G., Fang, Y. L., Comeau, D. S., Caldwell, P. M., Bartoletti, T., Balaguru, K., Taylor, M. A., McCoy, R. B., Leung, L. R., and Bader, D. C.: The DOE E3SM Model version 2: Overview of the physical model and initial model evaluation, Journal of Advances in Modeling Earth Systems, 14, e2022MS003156, https://doi.org/10.1029/2022MS003156, 2022.

Guo, Z., Dirmeyer, P. A., Delsole, T., and Koster, R. D.: Rebound in atmospheric predictability and the role of the land surface, Journal of Climate, 25(13), 4744–4749, https://doi.org/10.1175/JCLI-D-11-00651.1, 2012.

He, Y., Wang, B., Liu, M., Liu, L., Yu, Y., Liu, J., Li, R., Zhang, C., Xu, S., Huang, W., Liu, Q., Wang, Y., and Li, F.: Reduction of initial shock in decadal predictions using a new initialization strategy, Geophysical Research Letters, 44(16), 8538–8547, https://doi.org/10.1002/2017GL074028, 2017.

He, Y., Wang, B., Liu, L., Huang, W., Xu, S., Liu, J., Wang, Y., Li, L., Huang, X., Peng, Y., Lin, Y., and Yu, Y.: A DRP-4DVar-based coupled data assimilation system with a simplified off-line localization technique for decadal predictions, Journal of Advances in Modeling Earth Systems, 12(4), e2019MS001768, https://doi.org/10.1029/2019MS001768, 2020a.

He, Y., Wang, B., Huang, W., Xu, S., Wang, Y., Liu, L., Li, L., Liu, J., Yu, Y., Lin, Y., Huang, X., and Peng, Y.: A new DRP-4DVar-based coupled data assimilation system for decadal predictions using a fast online localization technique, Climate Dynamics, 54, 3541–3559, https://doi.org/10.1007/s00382-020-05190-w, 2020b.

Hoke, J. E. and Anthes, R. A.: The initialization of numerical models by a dynamic-initialization technique, Monthly Weather Review, 104(12), 1551–1556, https://doi.org/10.1175/1520-0493(1976)104<1551:TIONMB>2.0.CO;2, 1976.

Houborg, R., Rodell, M., Li, B., Reichle, R., and Zaitchik, B. F.: Drought indicators based on model-assimilated Gravity Recovery and Climate Experiment (GRACE) terrestrial water storage observations, Water Resources Research, 48, W07525, https://doi.org/10.1029/2011WR011291, 2012.

删除了： Hamill, T. A. and Snyder, C.: A hybrid ensemble Kalman filter-3D variational analysis scheme, Monthly Weather Review, 128, 2905–2919, https://doi.org/10.1175/1520-0493(2000)128<2905:AHEKFV>2.0.CO;2, 2000.

Kwon, Y., Yang, Z. L., Zhao, L., Hoar, T. J., Toure, A. M., and Rodell, M.: Estimating snow water storage in North America using CLM4, DART, and snow radiance data assimilation, Journal of Hydrometeorology, 17(11), 2853–2874, https://doi.org/10.1175/JHM-D-16-0028.1, 2016.

Laloyaux, P., Balmaseda, M., Dee, D., Mogensen, K., and Janssen, P.: A coupled data assimilation system for climate reanalysis, Quarterly Journal of the Royal Meteorological Society, 142(694), 65-78, https://doi.org/10.1002/qj.2629, 2016.

Lea, D. J., Mirouze, I., Martin, M. J., King, R. R., Hines, A., Walters, D., and Thurlow, M.: Assessing a new coupled data assimilation system based on the Met Office coupled atmosphere–land–ocean–sea ice model, Monthly Weather Review, 143(11), 4678-4694, https://doi.org/10.1175/MWR-D-15-0174.1, 2015.

Lei, L. L. and Hacker, J. P.: Nudging, ensemble, and nudging ensembles for data assimilation in the presence of model error, Monthly Weather Review, 143(7), 2600–2610, https://doi.org/10.1175/MWR-D-14-00295.1, 2015.

Leung, L. R., Bader, D. C., Taylor, M. A., and McCoy, R. B.: An introduction to the E3SM special collection: Goals, science drivers, development, and analysis, Journal of Advances in Modeling Earth Systems, 12(11), e2019MS001821, https://doi.org/10.1029/2019MS001821, 2020.

Li, F., Wang, B., He, Y., Huang, W., Xu, S., Liu, L., Liu, J. and Li, L.: Important role of North Atlantic air–sea coupling in the interannual predictability of summer precipitation over the eastern Tibetan Plateau, Climate Dynamics, 56, 1433–1448, https://doi.org/10.1007/s00382-020-05542-6, 2021.

Li, H. Y., Wigmosta, M. S., Wu, H., Huang, M., Ke, Y., Coleman, A. M., and Leung, L. R.: A physically based runoff routing model for land surface and Earth system models, Journal of Hydrometeorology, 14, 808–828, https://doi.org/10.1175/JHM-D-12-015.1, 2013.

Lin, L. F., Ebtehaj, A. M., Wang, J., and Bras, R. L.: Soil moisture background error covariance and data assimilation in a coupled land-atmosphere model, Water Resources Research, 53(2), 1309–1335, https://doi.org/10.1002/2015WR017548, 2017.

Lin, P., Yang, Z. L., Wei, J., Dickinson, R. E., Zhang, Y., and Zhao, L.: Assimilating multi-satellite snow data in ungauged Eurasia improves the simulation accuracy of Asian monsoon seasonal anomalies, Environmental Research Letters, 15(6), 064033, https://doi.org/10.1088/1748-9326/ab80ef, 2020.

Liu, D., and Mishra, A. K.: Performance of AMSR_E soil moisture data assimilation in CLM4. 5 model for monitoring hydrologic fluxes at global scale, Journal of Hydrometeorology, 547, 67–79, https://doi.org/10.1016/j.jhydrol.2017.01.036, 2017.

Liu, J. J., Wang, B., and Xiao, Q. N.: An evaluation study of the DRP-4-DVar approach with the Lorenz-96 model, Tellus A: Dynamic Meteorology and Oceanography, 63, 256–262, https://doi.org/10.1111/j.1600-0870.2010.00487.x, 2011.

Lorenc, A. C., Bowler, N. E., Clayton, A. M., Pring, S. R., and Fairbairn, D.: Comparison of hybrid-4DEnVar and hybrid-4DVar data assimilation methods for global NWP, Monthly Weather Review, 143, 212–229, https://doi.org/10.1175/MWR-D-14-00195.1, 2015.

Mochizuki, T., Masuda, S., Ishikawa, Y., and Awaji, T.: Multiyear climate prediction with initialization based on 4D-Var data assimilation, Geophysical Research Letters, 43(8), 3903–3910, https://doi.org/10.1002/2016GL067895, 2016.

Oleson, K. W., Lawrence, D. M., Bonan, G. B., Drewniak, B., Huang, M., Koven, C. D., Levis, S., Li, F., Riley, W. J., Subin, Z. M., Swenson, S. C., Thornton, P. E., Bozbiyik, A., Fisher, R., Heald, C. L., Kluzek, E., Lamarque, J. F., Lawrence, P. J., Leung, L. R., Lipscomb, W., Muszala, S., Ricciuto, D. M., Sacks, W., Sun, Y., Tang, J., and Yang, Z. L.: Technical description of version 4.5 of the Community Land Model (CLM) (Tech. Rep. NCAR/TN-503+STR). Boulder, Colorado, USA: National Center for Atmospheric Research, http://dx.doi.org/10.5065/D6RR1W7M, 2013.

Penny, S. G., and Hamill, T. M.: Coupled data assimilation for integrated earth system analysis and prediction, Bulletin of the American Meteorological Society, 98(7), ES169-ES172, https://doi.org/10.1175/BAMS-D-17-0036.1, 2017.

Penny, S. G., Bach, E., Bhargava, K., Chang, C. C., Da, C., Sun, L., and Yoshida, T.: Strongly coupled data assimilation in multiscale media: Experiments using a quasi-geostrophic coupled model, Journal of Advances in Modeling Earth Systems, 11(6), 1803-1829, https://doi.org/10.1029/2019MS001652, 2019.

Petersen, M., Asay-Davis, X. S., Jacobsen, D., Maltrud, M., Ringler, T., Van Roekel, L., and Wolfram, P.: MPAS ocean user's guide V6, Zenodo, https://doi.org/10.5281/zenodo.1246893, 2018.

Reckinger, S. M., Petersen, M. R., and Reckinger, S. J.: A study of overflow simulations using MPAS-

删除了： Liu, C., Xiao, Q. and Wang, B.: An ensemble-based four-dimensional variational data assimilation scheme. Part I: technical formulation and preliminary test, Monthly Weather Review, 136, 3363–3373, https://doi.org/10.1175/2008MWR2312.1, 2008.

删除了： Park, J. Y., Stock, C. A., Yang, X., Dunne, J. P., Rosati, A., John, J., and Zhang, S.: Modeling global ocean biogeochemistry with physical data assimilation: a pragmatic solution to the equatorial instability, Journal of Advances in modeling earth systems, 10(3), 891–906, https://doi.org/10.1002/2017MS001223, 2018.

删除了： Prodhomme, C., Doblas-Reyes, F., Bellprat, O., and Dutra, E.: Impact of land-surface initialization on sub-seasonal to seasonal forecasts over Europe, Climate dynamics, 47, 919–935, https://doi.org/10.1007/s00382-015-2879-4, 2016.

Ocean: Vertical grids, resolution, and viscosity, Ocean Modeling, 96, 291–313, https://doi.org/10.1016/j.ocemod.2015.09.006, 2015.

Rodell, M., Houser, P. R., Jambor, U., Gottschalck, J., Mitchell, K., Meng, C. J., Arsenault, K., Cosgrove, B., Radakovich, J., Bosilovich, M. and Entin, J. K., Walker, J. P., Lohmann, D., and Toll, D.: The global land data assimilation system, Bulletin of the American Meteorological society, 85(3), 381–394, https://doi.org/10.1175/BAMS-85-3-381, 2004.

Sakaguchi, K., Zeng, X., and Brunke, M. A.: The hindcast skill of the CMIP ensembles for the surface air temperature trend, Journal of Geophysical Research: Atmospheres, 117, D1611, https://doi.org/10.1029/2012JD017765, 2012.

Shi, P. F., Wang, B., He, Y., Lu, H., Yang, K., Xu, S. M., Huang, W. Y., Liu, L., Liu, J. J., Li, L. J., and Wang, Y.: Contributions of weakly coupled data assimilation–based land initialization to interannual predictability of summer climate over Europe, Journal of Climate, 35, 517–535, https://doi.org/10.1175/JCLI-D-20-0506.1, 2022.

Simmons, A. J. and Hollingsworth, A.: Some aspects of the improvement in skill of numerical weather prediction, Quarterly Journal of the Royal Meteorological Society, 128(580), 647–677, https://doi.org/10.1256/003590002321042135, 2002.

Smith, P. J., Fowler, A. M., and Lawless, A. S.: Exploring strategies for coupled 4DVar data assimilation using an idealised atmosphere–ocean model, Tellus A, 67(1):27025, https://doi.org/10.3402/tellusa.v67.27025, 2015.

Sluka, T. C., Penny, S. G., Kalnay, E., and Miyoshi, T.: Assimilating atmospheric observations into the ocean using strongly coupled ensemble data assimilation, Geophysical Research Letters, 43(2), 752-759, https://doi.org/10.1002/2015GL067238, 2016.

Sugiura, N., Awaji, T., Masuda, S., Mochizuki, T., Toyoda, T., Miyama, T., Igarashi, H. and Ishikawa, Y.: Development of a four-dimensional variational coupled data assimilation system for enhanced analysis and prediction of seasonal to interannual climate variations, Journal of Geophysical Research: Oceans, 113, C10017, https://doi.org/10.1029/2008JC004741, 2008.

Taylor, K. E., Stouffer, R. J., and Meehl, G. A.: An overview of CMIP5 and the experiment design, Bulletin of the American Meteorological Society, 93(4), 485–498, https://doi.org/10.1175/BAMS-

删除了： Santanello, J. A., Sujay V. K., Christa D. P., and Patricia M. L.: Impact of soil moisture assimilation on land surface model spin-up and coupled land-atmosphere prediction, Journal of Hydrometeorology, 17, 517–540, https://doi.org/10.1175/JHM-D-15-0072.1, 2016.

Shaffrey, L. C., Hodson, D., Robson, J., Stevens, D. P., Hawkins, E., Polo, I., Stevens, I., Sutton, R. T., Lister, G., Iwi, A. and Smith, D.: Decadal predictions with the HiGEM high resolution global coupled climate model: description and basic evaluation, Climate Dynamics, 48, 297–311, https://doi.org/10.1007/s00382-016-3075-x, 2017.

删除了： Smith, D. M., Eade, R., and Pohlmann, H.: A comparison of full-field and anomaly initialization for seasonal to decadal climate prediction, Climate Dynamics, 41(11), 3325–3338, https://doi.org/10.1007/s00382-013-1683-2, 2013.

D-11-00094.1, 2012.

Taylor, M. A., Guba, O., Steyer, A., Ullrich, P. A., Hall, D. M., and Eldrid, C.: An energy consistent discretization of the nonhydrostatic equations in primitive variables, Journal of Advances in Modeling Earth Systems, 12, e2019MS001783, https://doi.org/10.1029/2019MS001783, 2020.

Wang, B., Liu, J., Wang, S., Cheng, W., Liu, J., Liu, C., Xiao, Q., and Kuo, Y. H.: An economical approach to four-dimensional variational data assimilation, Advances in Atmospheric Sciences, 27, 715–727, https://doi.org/10.1007/s00376-009-9122-3, 2010.

Wang, B., Liu, J., Liu, L., Xu, S., and Huang, W.: An approach to localization for ensemble-based data assimilation, PloS one, 13(1), e0191088, https://doi.org/10.1371/journal.pone.0191088, 2018.

Wang, G., Dolman, A. J., Blender, R., and Fraedrich, K.: Fluctuation regimes of soil moisture in ERA-40 reanalysis data, Theoretical and Applied Climatology, 99, 1–8, https://doi.org/10.1007/s00704-009-0111-3, 2010.

Yao, Y., Luo, Y., Huang, J., and Ma, J.: Improving the downscaled springtime temperature in Central Asia through assimilating meteorological and snow cover observations, Atmospheric Research, 258, 105619, https://doi.org/10.1016/j.atmosres.2021.105619, 2021.

Yin, J., Zhan, X., Zheng, Y., Liu, J., Hain, C. R., and Fang, L.: Impact of quality control of satellite soil moisture data on their assimilation into land surface model, Geophysical Research Letters, 41(20), 7159–7166, https://doi.org/10.1002/2014GL060659, 2014.

Yoshida, T., and Kalnay, E.: Correlation-cutoff method for covariance localization in strongly coupled data assimilation, Monthly Weather Review, 146(9), 2881-2889, https://doi.org/10.1175/MWR-D-17-0365.1, 2018.

Zeng, X., and Decker, M.: Improving the numerical solution of soil moisture–based Richards equation for land models with a deep or shallow water table, Journal of Hydrometeorology, 10, 308–319, https://doi.org/10.1175/2008JHM1011.1, 2009.

Zhang, H., Zhang, L. L., Li, J., An, R. D., Deng, Y.: Climate and Hydrological Change Characteristics and Applicability of GLDAS Data in the Yarlung Zangbo River Basin, China, Water, 10, 254, https://doi.org/10.3390/w10030254, 2018.

Zhang, S., Harrison, M. J., Wittenberg, A. T., Rosati, A., Anderson, J. L., and Balaji, V.: Initialization of

删除了： Timouk, F., Kergoat, L., Mougin, É., Lloyd, C. R., Ceschia, E., Cohard, J. M., De Rosnay, P., Hiernaux, P., Demarez, V. and Taylor, C.M.: Response of surface energy balance to water regime and vegetation development in a Sahelian landscape, Journal of Hydrometeorology, 375, 178–189, https://doi.org/10.1016/j.jhydrol.2009.04.022, 2009.

删除了： Wang, X., Baker, D. M., Snyder, C. and Hamill, T. M.: A hybrid ETKF-3DVAR data assimilation scheme for the WRF model. Part I: observing system simulation experiment, Monthly Weather Review, 136, 5116–5131, https://doi.org/10.1175/2008MWR2444.1, 2008.
Wei, M., Li, Q., Xin, X., Zhou, W., Han, Z., Luo, Y., and Zhao, Z.: Improved decadal climate prediction in the North Atlantic using EnOI-assimilated initial condition, Science Bulletin, 62(16), 1142–1147, https://doi.org/10.1016/j.scib.2017.08.012, 2017.
Wu, B., Zhou, T., and Zheng, F.: EnOI-IAU initialization scheme designed for decadal climate prediction system IAP-DecPreS, Journal of Advances in Modeling Earth Systems, 10(2), 342–356, https://doi.org/10.1002/2017MS001132, 2018.

an ENSO forecast system using a parallelized ensemble filter, Monthly Weather Review, 133(11), 3176-3201, https://doi.org/10.1175/MWR3024.1, 2005.

Zhang, S., Harrison, M. J., Rosati, A., and Wittenberg, A.: System design and evaluation of coupled ensemble data assimilation for global oceanic climate studies, Monthly Weather Review, 135(10), 3541-3564, https://doi.org/10.1175/MWR3466.1, 2007.

Zhang, S., Liu, Z., Zhang, X., Wu, X., Han, G., Zhao, Y., Yu, X., Liu, C., Liu, Y., Wu, S., Lu, F., Li, M., Deng, X.: Coupled data assimilation and parameter estimation in coupled ocean–atmosphere models: a review, Climate Dynamics, 54, 5127-5144, https://doi.org/10.1007/s00382-020-05275-6, 2020.

Zhou, J., Yang, K., Crow, W.T., Dong, J., Zhao, L., Feng, H., Zou, M., Lu, H., Tang, R. and Jiang, Y.: Potential of remote sensing surface temperature-and evapotranspiration-based land-atmosphere coupling metrics for land surface model calibration, Remote Sensing of Environment, 291, 113557, https://doi.org/10.1016/j.rse.2023.113557, 2023.

删除了： Zhang, Y. F., Hoar, T. J., Yang, Z. L., Anderson, J. L., Toure, A. M., and Rodell, M.: Assimilation of MODIS snow cover through the Data Assimilation Research Testbed and the Community Land Model version 4, Journal of Geophysical Research: Atmospheres, 119(12), 7091–7103, https://doi.org/10.1002/2013JD021329, 2014.

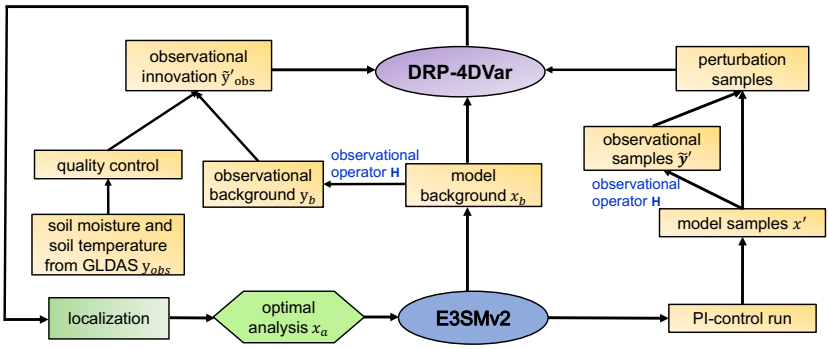

Figure 1. Flowchart of the 4DEnVar-based WCLDA system in E3SMv2 based on the DRP-4DVar method.

删除了：LCDA

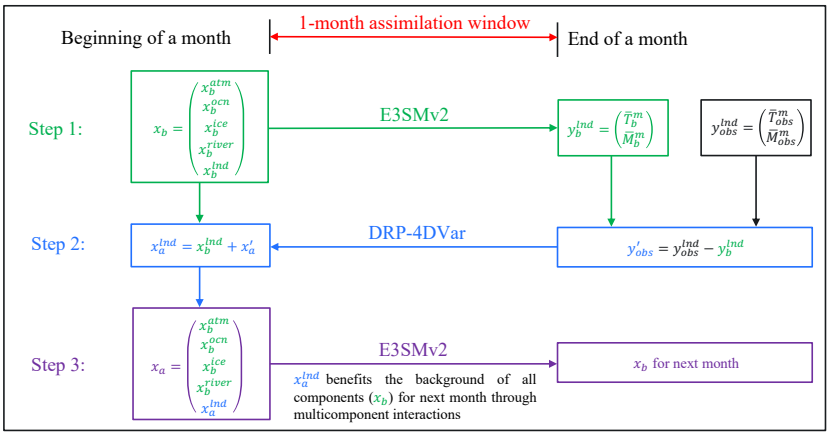

Figure 2. Schematic flowchart of the 4DEnVar-based WCLDA system. The beginning of a month is at 0000 UTC on the first day of the month, and the end of the month is at 0000 UTC on the first day of the next month. x_b denotes the background vector including the backgrounds of all E3SMv2 components (atmosphere (x_b^{atm}), ocean (x_b^{ocn}), sea ice (x_b^{ice}), river transport (x_b^{river}) and land surface (x_b^{lnd})). x_a consists of the assimilation analysis of land surface (x_a^{lnd}) and the backgrounds of other components. y_b^{lnd} represents the simulated monthly mean soil temperature (T_b^m) and moisture (M_b^m) by E3SMv2 using x_b as the initial condition. y_{obs}^{lnd} denotes the monthly mean GLDAS data of soil temperature (T_{obs}^m) and moisture (M_{obs}^m). y'_{obs} denotes the observational innovation, which is the difference between the GLDAS data (y_{obs}^{lnd}) and the observational background (y_b^{lnd}).

删除了：LCDA

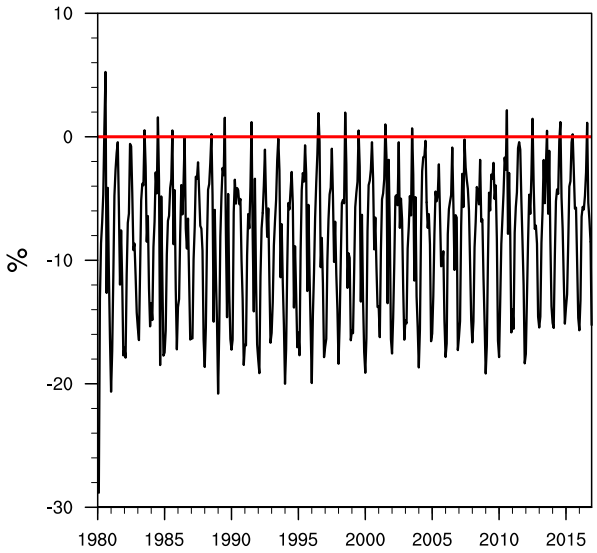

Figure 3. Time series of the reduction rate of the cost function from 1980 to 2016 in the 4DEnVar-based WCLDA system.

删除了：LCDA

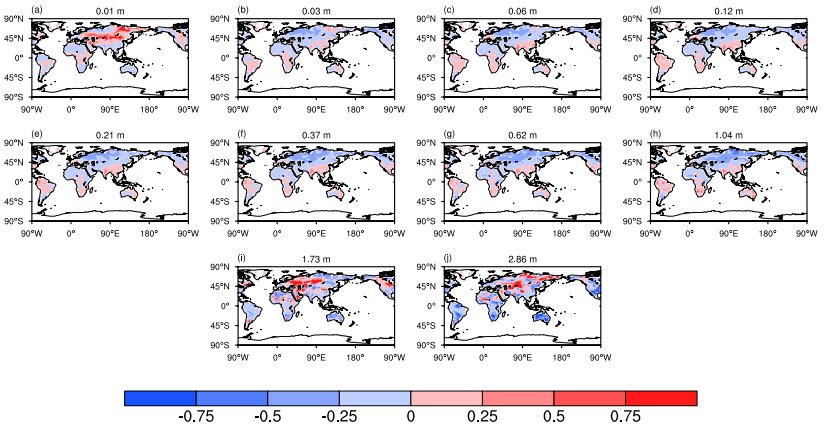

1156

1157 **Figure 4.** Spatial distribution of the AE index for soil moisture from the surface to deep layers during

1158 the 1980-2016 period. The number at the top center denotes the depth of each soil layer.

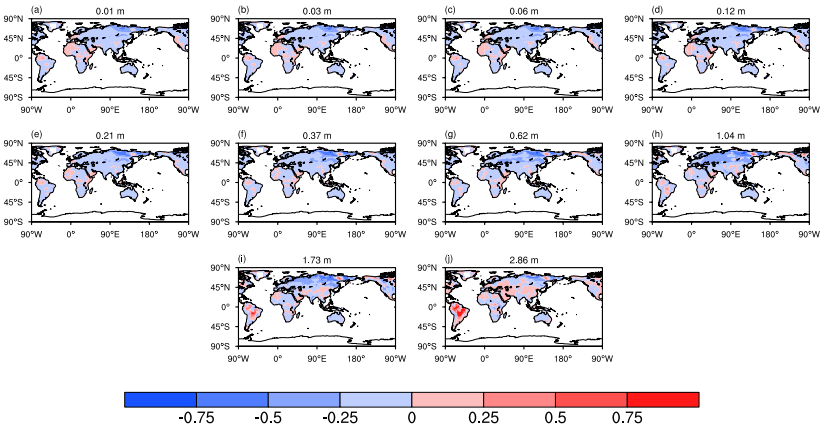

Figure 5. Same as in Figure 4, but for soil temperature.

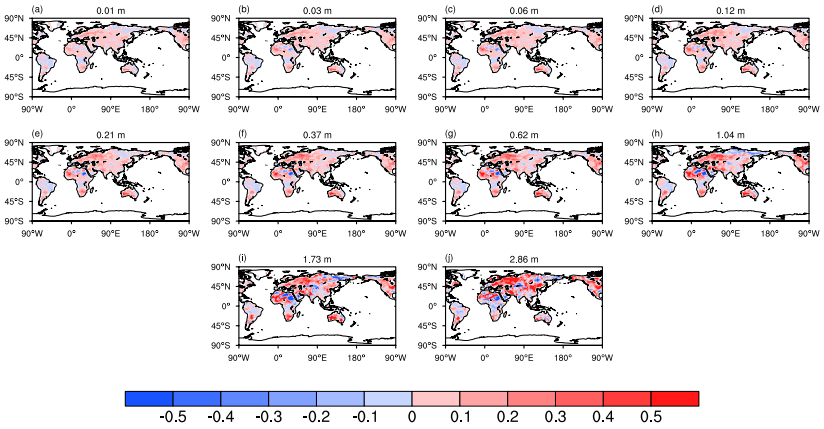

1161

1162 **Figure 6.** Differences between correlations of soil moisture in Assim and CTRL with the GLDAS data
1163 from the surface to deep layers for the period of 1980-2016. The number at the top center denotes the
1164 depth of each soil layer.

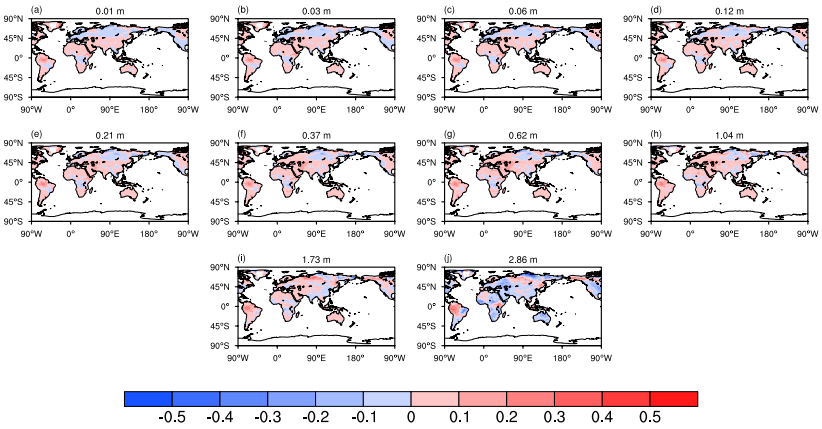

1165

1166 **Figure 7.** Same as in Figure 6, but for soil temperature.

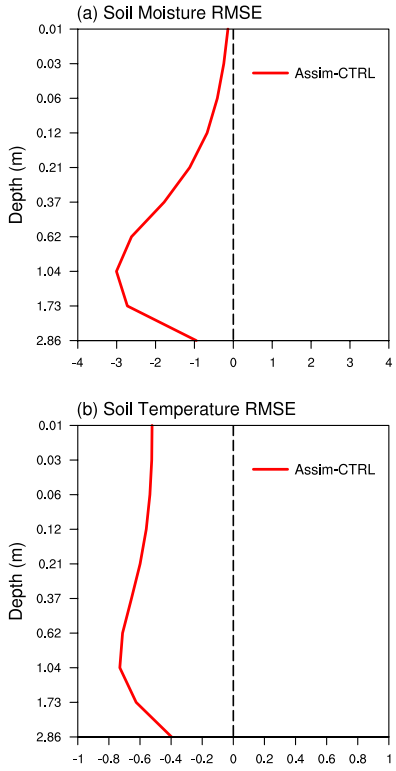

1167

1168 **Figure 8.** Vertical distributions of RMSE differences (Assim minus CTRL) for (a) soil moisture and (b)

1169 soil temperature averaged over the global land and throughout 1980-2016.

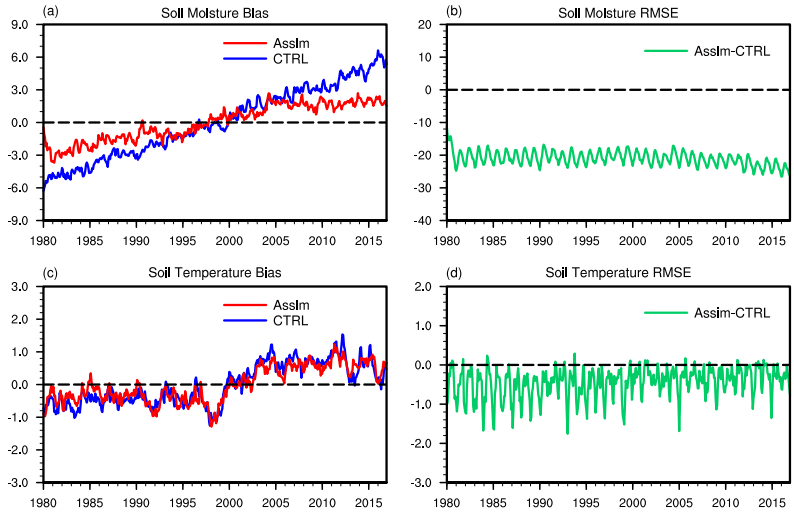

Figure 9. Time series of the vertically averaged global mean soil moisture and temperature bias (left) for Assim (red line) and CTRL (blue line), and RMSE differences (right, green line) between Assim and CTRL from 1980 to 2016.

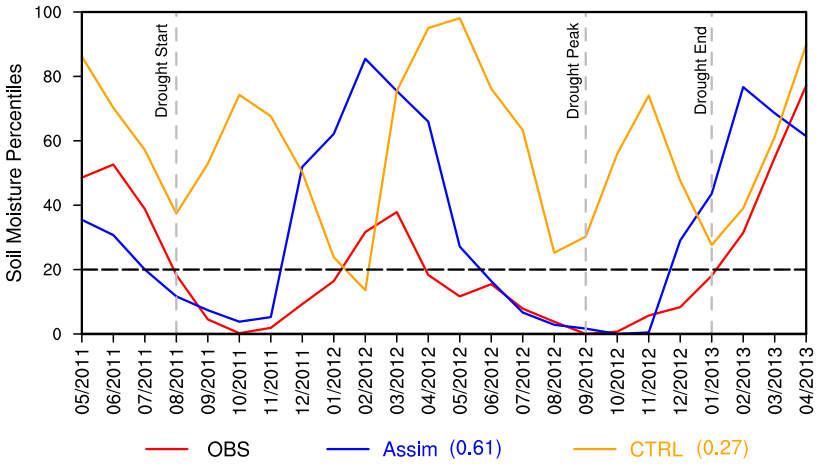

1174

1175 **Figure 10.** Time series of soil moisture percentiles between May 2011 and April 2013 during the 2012
1176 U.S. Midwest drought. Red line: observation, blue line: Assim, orange line: CTRL. The correlation
1177 coefficients between Assim and CTRL with observations are also shown. The three vertical dashed lines
1178 mark the timing of drought start, drought peak and drought end, respectively. The start of the agricultural
1179 drought is defined as the month when soil moisture falls below the 20th percentile. The soil moisture
1180 percentiles are averaged over the U.S. Midwest (36°-50°N, 102°-88°W). The observed soil moisture is
1181 derived from ERA-Interim monthly soil moisture data.

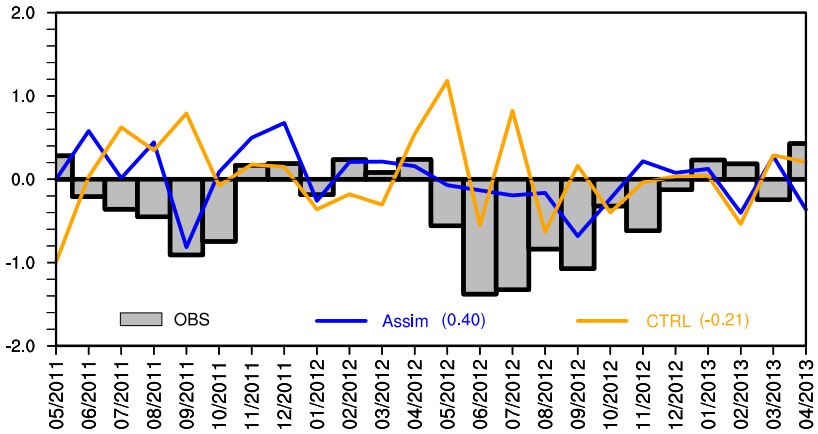

Figure 11. Time series of precipitation anomaly over the Midwest between May 2011 and April 2013 during the 2012 U.S. Midwest drought. Gray bar: observation, blue line: Assim, orange line: CTRL. The precipitation anomalies are calculated by removing the annual cycle and the long-term trend. The correlation coefficients of Assim and CTRL with observation are also shown. The precipitation anomalies are averaged over the U.S. Midwest (36°-50°N, 102°-88°W). The observed precipitation is derived from GPCP monthly precipitation data.

第 5 页: [1] 删除了 Shi, Pengfei 2023/11/22 20:40:00

第 5 页: [2] 删除了 Shi, Pengfei 2023/10/16 11:01:00

第 8 页: [3] 设置了格式 Shi, Pengfei 2023/11/22 11:29:00

字体颜色: 文字 1

第 8 页: [3] 设置了格式 Shi, Pengfei 2023/11/22 11:29:00

字体颜色: 文字 1

第 8 页: [3] 设置了格式 Shi, Pengfei 2023/11/22 11:29:00

字体颜色: 文字 1

第 8 页: [4] 设置了格式 Shi, Pengfei 2023/11/22 11:29:00

字体颜色: 文字 1

第 8 页: [4] 设置了格式 Shi, Pengfei 2023/11/22 11:29:00

字体颜色: 文字 1

第 8 页: [5] 设置了格式 Shi, Pengfei 2023/11/22 11:29:00

字体颜色: 文字 1

第 8 页: [5] 设置了格式 Shi, Pengfei 2023/11/22 11:29:00

字体颜色: 文字 1

第 8 页: [5] 设置了格式 Shi, Pengfei 2023/11/22 11:29:00

字体颜色: 文字 1

第 8 页: [5] 设置了格式 Shi, Pengfei 2023/11/22 11:29:00

字体颜色: 文字 1

第 8 页: [5] 设置了格式 Shi, Pengfei 2023/11/22 11:29:00

字体颜色: 文字 1

第 8 页: [5] 设置了格式 Shi, Pengfei 2023/11/22 11:29:00

字体颜色: 文字 1

第 8 页: [5] 设置了格式 Shi, Pengfei 2023/11/22 11:29:00

字体颜色: 文字 1

第 8 页: [5] 设置了格式 Shi, Pengfei 2023/11/22 11:29:00

字体颜色: 文字 1

第 8 页: [5] 设置了格式 Shi, Pengfei 2023/11/22 11:29:00

字体颜色: 文字 1

第 8 页: [6] 设置了格式 Shi, Pengfei 2023/11/22 11:29:00

字体颜色: 文字 1

第 8 页: [6] 设置了格式 Shi, Pengfei 2023/11/22 11:29:00

字体颜色: 文字 1

第 8 页: [6] 设置了格式 Shi, Pengfei 2023/11/22 11:29:00

字体颜色: 文字 1

第 8 页: [6] 设置了格式 Shi, Pengfei 2023/11/22 11:29:00

字体颜色: 文字 1

第 8 页: [6] 设置了格式 Shi, Pengfei 2023/11/22 11:29:00

字体颜色: 文字 1

第 8 页: [6] 设置了格式 Shi, Pengfei 2023/11/22 11:29:00

字体颜色: 文字 1

第 8 页: [6] 设置了格式 Shi, Pengfei 2023/11/22 11:29:00

字体颜色: 文字 1

第 8 页: [6] 设置了格式 Shi, Pengfei 2023/11/22 11:29:00

字体颜色: 文字 1

第 8 页: [6] 设置了格式 Shi, Pengfei 2023/11/22 11:29:00

字体颜色: 文字 1

第 8 页: [7] 设置了格式 Shi, Pengfei 2023/11/22 11:29:00

字体颜色: 文字 1

第 8 页: [7] 设置了格式 Shi, Pengfei 2023/11/22 11:29:00

字体颜色: 文字 1

第 8 页: [8] 设置了格式 Shi, Pengfei 2023/11/22 11:29:00

字体颜色: 文字 1

第 8 页: [8] 设置了格式 Shi, Pengfei 2023/11/22 11:29:00

字体颜色: 文字 1

第 8 页: [9] 设置了格式 Shi, Pengfei 2023/11/22 11:29:00

字体颜色: 文字 1

第 8 页: [9] 设置了格式 Shi, Pengfei 2023/11/22 11:29:00

字体颜色: 文字 1

第 8 页: [10] 设置了格式 Shi, Pengfei 2023/11/22 11:29:00

字体颜色: 文字 1

第 8 页: [10] 设置了格式　Shi, Pengfei　2023/11/22 11:29:00

字体颜色: 文字 1

第 8 页: [10] 设置了格式　Shi, Pengfei　2023/11/22 11:29:00

字体颜色: 文字 1

第 8 页: [11] 设置了格式　Shi, Pengfei　2023/11/22 11:29:00

字体颜色: 文字 1

第 8 页: [11] 设置了格式　Shi, Pengfei　2023/11/22 11:29:00

字体颜色: 文字 1

第 8 页: [11] 设置了格式　Shi, Pengfei　2023/11/22 11:29:00

字体颜色: 文字 1

第 8 页: [11] 设置了格式　Shi, Pengfei　2023/11/22 11:29:00

字体颜色: 文字 1

第 8 页: [11] 设置了格式　Shi, Pengfei　2023/11/22 11:29:00

字体颜色: 文字 1

第 8 页: [11] 设置了格式　Shi, Pengfei　2023/11/22 11:29:00

字体颜色: 文字 1

第 8 页: [11] 设置了格式　Shi, Pengfei　2023/11/22 11:29:00

字体颜色: 文字 1

第 8 页: [11] 设置了格式 Shi, Pengfei 2023/11/22 11:29:00

字体颜色: 文字 1

第 8 页: [11] 设置了格式 Shi, Pengfei 2023/11/22 11:29:00

字体颜色: 文字 1

第 8 页: [11] 设置了格式 Shi, Pengfei 2023/11/22 11:29:00

字体颜色: 文字 1

第 8 页: [11] 设置了格式 Shi, Pengfei 2023/11/22 11:29:00

字体颜色: 文字 1

第 8 页: [11] 设置了格式 Shi, Pengfei 2023/11/22 11:29:00

字体颜色: 文字 1

第 8 页: [11] 设置了格式 Shi, Pengfei 2023/11/22 11:29:00

字体颜色: 文字 1

第 8 页: [11] 设置了格式 Shi, Pengfei 2023/11/22 11:29:00

字体颜色: 文字 1

第 8 页: [11] 设置了格式 Shi, Pengfei 2023/11/22 11:29:00

字体颜色: 文字 1

第 8 页: [11] 设置了格式　Shi, Pengfei　2023/11/22 11:29:00

字体颜色: 文字 1

第 8 页: [12] 设置了格式　Shi, Pengfei　2023/11/22 11:29:00

字体颜色: 文字 1

第 8 页: [12] 设置了格式　Shi, Pengfei　2023/11/22 11:29:00

字体颜色: 文字 1

第 8 页: [12] 设置了格式　Shi, Pengfei　2023/11/22 11:29:00

字体颜色: 文字 1

第 8 页: [12] 设置了格式　Shi, Pengfei　2023/11/22 11:29:00

字体颜色: 文字 1

第 8 页: [12] 设置了格式　Shi, Pengfei　2023/11/22 11:29:00

字体颜色: 文字 1

第 8 页: [12] 设置了格式　Shi, Pengfei　2023/11/22 11:29:00

字体颜色: 文字 1

第 8 页: [12] 设置了格式　Shi, Pengfei　2023/11/22 11:29:00

字体颜色: 文字 1

第 8 页: [12] 设置了格式　Shi, Pengfei　2023/11/22 11:29:00

字体颜色: 文字 1

第 8 页: [12] 设置了格式 Shi, Pengfei 2023/11/22 11:29:00

字体颜色: 文字 1

第 8 页: [12] 设置了格式 Shi, Pengfei 2023/11/22 11:29:00

字体颜色: 文字 1

第 8 页: [12] 设置了格式 Shi, Pengfei 2023/11/22 11:29:00

字体颜色: 文字 1

第 8 页: [12] 设置了格式 Shi, Pengfei 2023/11/22 11:29:00

字体颜色: 文字 1

第 8 页: [12] 设置了格式 Shi, Pengfei 2023/11/22 11:29:00

字体颜色: 文字 1

第 8 页: [12] 设置了格式 Shi, Pengfei 2023/11/22 11:29:00

字体颜色: 文字 1

第 8 页: [12] 设置了格式 Shi, Pengfei 2023/11/22 11:29:00

字体颜色: 文字 1

第 8 页: [12] 设置了格式 Shi, Pengfei 2023/11/22 11:29:00

字体颜色: 文字 1

第 8 页: [13] 设置了格式 Shi, Pengfei 2023/11/22 11:29:00

字体颜色: 文字 1

第 8 页: [13] 设置了格式 Shi, Pengfei 2023/11/22 11:29:00

字体颜色: 文字 1

第 8 页: [13] 设置了格式 Shi, Pengfei 2023/11/22 11:29:00

字体颜色: 文字 1

第 8 页: [13] 设置了格式 Shi, Pengfei 2023/11/22 11:29:00

字体颜色: 文字 1

第 8 页: [14] 设置了格式 Shi, Pengfei 2023/11/22 11:29:00

字体颜色: 文字 1

第 8 页: [14] 设置了格式 Shi, Pengfei 2023/11/22 11:29:00

字体颜色: 文字 1

第 8 页: [14] 设置了格式 Shi, Pengfei 2023/11/22 11:29:00

字体颜色: 文字 1

第 8 页: [14] 设置了格式 Shi, Pengfei 2023/11/22 11:29:00

字体颜色: 文字 1

第 8 页: [14] 设置了格式 Shi, Pengfei 2023/11/22 11:29:00

字体颜色: 文字 1

第 8 页: [14] 设置了格式 Shi, Pengfei 2023/11/22 11:29:00

字体颜色: 文字 1

第 8 页: [14] 设置了格式 Shi, Pengfei 2023/11/22 11:29:00

字体颜色: 文字 1

第 8 页: [14] 设置了格式 Shi, Pengfei 2023/11/22 11:29:00

字体颜色: 文字 1

第 8 页: [14] 设置了格式 Shi, Pengfei 2023/11/22 11:29:00

字体颜色: 文字 1

第 8 页: [14] 设置了格式 Shi, Pengfei 2023/11/22 11:29:00

字体颜色: 文字 1

第 8 页: [15] 设置了格式 Shi, Pengfei 2023/11/22 11:29:00

字体颜色: 文字 1

第 8 页: [15] 设置了格式 Shi, Pengfei 2023/11/22 11:29:00

字体颜色: 文字 1

第 8 页: [15] 设置了格式 Shi, Pengfei 2023/11/22 11:29:00

字体颜色: 文字 1

第 8 页: [16] 设置了格式 Shi, Pengfei 2023/11/22 11:29:00

字体颜色: 文字 1

第 8 页: [16] 设置了格式 Shi, Pengfei 2023/11/22 11:29:00

字体颜色: 文字 1

第 8 页: [16] 设置了格式 Shi, Pengfei 2023/11/22 11:29:00

字体颜色: 文字 1

第 8 页: [17] 设置了格式 Shi, Pengfei 2023/11/22 11:29:00

字体颜色: 文字 1

第 8 页: [17] 设置了格式 Shi, Pengfei 2023/11/22 11:29:00

字体颜色: 文字 1

第 8 页: [17] 设置了格式 Shi, Pengfei 2023/11/22 11:29:00

字体颜色: 文字 1

第 8 页: [17] 设置了格式 Shi, Pengfei 2023/11/22 11:29:00

字体颜色: 文字 1

第 8 页: [18] 设置了格式 Shi, Pengfei 2023/11/22 11:29:00

字体颜色: 文字 1

第 8 页: [18] 设置了格式 Shi, Pengfei 2023/11/22 11:29:00

字体颜色: 文字 1

第 8 页: [18] 设置了格式 Shi, Pengfei 2023/11/22 11:29:00

字体颜色: 文字 1

第 8 页: [18] 设置了格式 Shi, Pengfei 2023/11/22 11:29:00

字体颜色: 文字 1

第 8 页: [18] 设置了格式 Shi, Pengfei 2023/11/22 11:29:00

字体颜色: 文字 1

第 8 页: [18] 设置了格式 Shi, Pengfei 2023/11/22 11:29:00

字体颜色: 文字 1

第 8 页: [19] 设置了格式 Shi, Pengfei 2023/11/22 11:29:00

字体颜色: 文字 1

第 8 页: [19] 设置了格式 Shi, Pengfei 2023/11/22 11:29:00

字体颜色: 文字 1

第 8 页: [19] 设置了格式 Shi, Pengfei 2023/11/22 11:29:00

字体颜色: 文字 1

第 8 页: [19] 设置了格式 Shi, Pengfei 2023/11/22 11:29:00

字体颜色: 文字 1

第 8 页: [20] 设置了格式 Shi, Pengfei 2023/11/22 11:29:00

字体颜色: 文字 1

第 8 页: [20] 设置了格式 Shi, Pengfei 2023/11/22 11:29:00

字体颜色: 文字 1

第 8 页: [20] 设置了格式 Shi, Pengfei 2023/11/22 11:29:00

字体颜色: 文字 1

第 8 页: [20] 设置了格式 Shi, Pengfei 2023/11/22 11:29:00

字体颜色: 文字 1

第 8 页: [20] 设置了格式 Shi, Pengfei 2023/11/22 11:29:00

字体颜色: 文字 1

第 8 页: [20] 设置了格式 Shi, Pengfei 2023/11/22 11:29:00

字体颜色: 文字 1

第 8 页: [20] 设置了格式 Shi, Pengfei 2023/11/22 11:29:00

字体颜色: 文字 1

第 8 页: [20] 设置了格式 Shi, Pengfei 2023/11/22 11:29:00

字体颜色: 文字 1

第 8 页: [20] 设置了格式 Shi, Pengfei 2023/11/22 11:29:00

字体颜色: 文字 1

第 8 页: [20] 设置了格式 Shi, Pengfei 2023/11/22 11:29:00

字体颜色: 文字 1

第 8 页: [20] 设置了格式 Shi, Pengfei 2023/11/22 11:29:00

字体颜色: 文字 1

第 8 页: [20] 设置了格式 Shi, Pengfei 2023/11/22 11:29:00

字体颜色: 文字 1

第 8 页: [20] 设置了格式 Shi, Pengfei 2023/11/22 11:29:00

字体颜色: 文字 1

第 8 页: [20] 设置了格式 Shi, Pengfei 2023/11/22 11:29:00

字体颜色: 文字 1

第 8 页: [20] 设置了格式 Shi, Pengfei 2023/11/22 11:29:00

字体颜色: 文字 1

第 8 页: [20] 设置了格式 Shi, Pengfei 2023/11/22 11:29:00

字体颜色: 文字 1

第 8 页: [21] 设置了格式 Shi, Pengfei 2023/11/22 11:29:00

字体颜色: 文字 1

第 8 页: [21] 设置了格式 Shi, Pengfei 2023/11/22 11:29:00

字体颜色: 文字 1

第 8 页: [21] 设置了格式　Shi, Pengfei　2023/11/22 11:29:00

字体颜色: 文字 1

第 8 页: [22] 设置了格式　Shi, Pengfei　2023/11/22 11:29:00

字体颜色: 文字 1

第 8 页: [22] 设置了格式　Shi, Pengfei　2023/11/22 11:29:00

字体颜色: 文字 1

第 8 页: [22] 设置了格式　Shi, Pengfei　2023/11/22 11:29:00

字体颜色: 文字 1

第 8 页: [22] 设置了格式　Shi, Pengfei　2023/11/22 11:29:00

字体颜色: 文字 1

第 8 页: [22] 设置了格式　Shi, Pengfei　2023/11/22 11:29:00

字体颜色: 文字 1

第 8 页: [22] 设置了格式　Shi, Pengfei　2023/11/22 11:29:00

字体颜色: 文字 1

第 8 页: [22] 设置了格式　Shi, Pengfei　2023/11/22 11:29:00

字体颜色: 文字 1

第 8 页: [22] 设置了格式　Shi, Pengfei　2023/11/22 11:29:00

字体颜色: 文字 1

第 8 页: [22] 设置了格式 Shi, Pengfei 2023/11/22 11:29:00

字体颜色: 文字 1

第 8 页: [22] 设置了格式 Shi, Pengfei 2023/11/22 11:29:00

字体颜色: 文字 1

第 8 页: [22] 设置了格式 Shi, Pengfei 2023/11/22 11:29:00

字体颜色: 文字 1

第 8 页: [22] 设置了格式 Shi, Pengfei 2023/11/22 11:29:00

字体颜色: 文字 1

第 8 页: [22] 设置了格式 Shi, Pengfei 2023/11/22 11:29:00

字体颜色: 文字 1

第 8 页: [22] 设置了格式 Shi, Pengfei 2023/11/22 11:29:00

字体颜色: 文字 1

第 8 页: [22] 设置了格式 Shi, Pengfei 2023/11/22 11:29:00

字体颜色: 文字 1

第 8 页: [23] 设置了格式 Shi, Pengfei 2023/11/22 11:29:00

字体颜色: 文字 1

第 8 页: [23] 设置了格式 Shi, Pengfei 2023/11/22 11:29:00

字体颜色: 文字 1

第 8 页: [23] 设置了格式 Shi, Pengfei 2023/11/22 11:29:00

字体颜色: 文字 1

第 8 页: [24] 设置了格式 Shi, Pengfei 2023/11/22 11:29:00

字体颜色: 文字 1

第 8 页: [24] 设置了格式 Shi, Pengfei 2023/11/22 11:29:00

字体颜色: 文字 1

第 8 页: [24] 设置了格式 Shi, Pengfei 2023/11/22 11:29:00

字体颜色: 文字 1

第 8 页: [25] 设置了格式 Shi, Pengfei 2023/11/22 11:29:00

字体颜色: 文字 1

第 8 页: [25] 设置了格式 Shi, Pengfei 2023/11/22 11:29:00

字体颜色: 文字 1

第 8 页: [25] 设置了格式 Shi, Pengfei 2023/11/22 11:29:00

字体颜色: 文字 1

第 8 页: [26] 设置了格式 Shi, Pengfei 2023/11/22 11:29:00

字体颜色: 文字 1

第 8 页: [26] 设置了格式 Shi, Pengfei 2023/11/22 11:29:00

字体颜色: 文字 1

第 8 页: [26] 设置了格式 Shi, Pengfei 2023/11/22 11:29:00

字体颜色: 文字 1

第 8 页: [26] 设置了格式 Shi, Pengfei 2023/11/22 11:29:00

字体颜色: 文字 1

第 8 页: [26] 设置了格式 Shi, Pengfei 2023/11/22 11:29:00

字体颜色: 文字 1

第 8 页: [26] 设置了格式 Shi, Pengfei 2023/11/22 11:29:00

字体颜色: 文字 1

第 8 页: [26] 设置了格式 Shi, Pengfei 2023/11/22 11:29:00

字体颜色: 文字 1

第 8 页: [26] 设置了格式 Shi, Pengfei 2023/11/22 11:29:00

字体颜色: 文字 1

第 8 页: [26] 设置了格式 Shi, Pengfei 2023/11/22 11:29:00

字体颜色: 文字 1

第 8 页: [26] 设置了格式 Shi, Pengfei 2023/11/22 11:29:00

字体颜色: 文字 1

第 8 页: [26] 设置了格式 Shi, Pengfei 2023/11/22 11:29:00

字体颜色: 文字 1

第 8 页: [26] 设置了格式 Shi, Pengfei 2023/11/22 11:29:00

字体颜色: 文字 1

第 8 页: [26] 设置了格式 Shi, Pengfei 2023/11/22 11:29:00

字体颜色: 文字 1

第 8 页: [26] 设置了格式 Shi, Pengfei 2023/11/22 11:29:00

字体颜色: 文字 1

第 8 页: [26] 设置了格式 Shi, Pengfei 2023/11/22 11:29:00

字体颜色: 文字 1

第 8 页: [27] 设置了格式 Shi, Pengfei 2023/11/22 11:29:00

字体颜色: 文字 1

第 8 页: [27] 设置了格式 Shi, Pengfei 2023/11/22 11:29:00

字体颜色: 文字 1

第 8 页: [27] 设置了格式 Shi, Pengfei 2023/11/22 11:29:00

字体颜色: 文字 1

第 8 页: [27] 设置了格式 Shi, Pengfei 2023/11/22 11:29:00

字体颜色: 文字 1

第 8 页: [27] 设置了格式　Shi, Pengfei　2023/11/22 11:29:00

字体颜色: 文字 1

第 8 页: [27] 设置了格式　Shi, Pengfei　2023/11/22 11:29:00

字体颜色: 文字 1

第 8 页: [27] 设置了格式　Shi, Pengfei　2023/11/22 11:29:00

字体颜色: 文字 1

第 8 页: [27] 设置了格式　Shi, Pengfei　2023/11/22 11:29:00

字体颜色: 文字 1

第 8 页: [27] 设置了格式　Shi, Pengfei　2023/11/22 11:29:00

字体颜色: 文字 1

第 8 页: [27] 设置了格式　Shi, Pengfei　2023/11/22 11:29:00

字体颜色: 文字 1

第 8 页: [27] 设置了格式　Shi, Pengfei　2023/11/22 11:29:00

字体颜色: 文字 1

第 8 页: [27] 设置了格式　Shi, Pengfei　2023/11/22 11:29:00

字体颜色: 文字 1

第 8 页: [28] 设置了格式 Shi, Pengfei 2023/11/22 11:29:00

字体颜色: 文字 1

第 8 页: [28] 设置了格式 Shi, Pengfei 2023/11/22 11:29:00

字体颜色: 文字 1

第 8 页: [28] 设置了格式 Shi, Pengfei 2023/11/22 11:29:00

字体颜色: 文字 1

第 8 页: [29] 设置了格式 Shi, Pengfei 2023/11/22 11:29:00

字体颜色: 文字 1

第 8 页: [29] 设置了格式 Shi, Pengfei 2023/11/22 11:29:00

字体颜色: 文字 1

第 8 页: [29] 设置了格式 Shi, Pengfei 2023/11/22 11:29:00

字体颜色: 文字 1

第 9 页: [30] 设置了格式 Shi, Pengfei 2023/11/22 11:29:00

字体颜色: 文字 1

第 9 页: [30] 设置了格式 Shi, Pengfei 2023/11/22 11:29:00

字体颜色: 文字 1

第 9 页: [30] 设置了格式 Shi, Pengfei 2023/11/22 11:29:00

字体颜色: 文字 1

第 9 页: [30] 设置了格式 Shi, Pengfei 2023/11/22 11:29:00

字体颜色: 文字 1

第 9 页: [30] 设置了格式 Shi, Pengfei 2023/11/22 11:29:00

字体颜色: 文字 1

第 9 页: [30] 设置了格式 Shi, Pengfei 2023/11/22 11:29:00

字体颜色: 文字 1

第 9 页: [30] 设置了格式 Shi, Pengfei 2023/11/22 11:29:00

字体颜色: 文字 1

第 9 页: [30] 设置了格式 Shi, Pengfei 2023/11/22 11:29:00

字体颜色: 文字 1

第 9 页: [30] 设置了格式 Shi, Pengfei 2023/11/22 11:29:00

字体颜色: 文字 1

第 9 页: [30] 设置了格式 Shi, Pengfei 2023/11/22 11:29:00

字体颜色: 文字 1

第 9 页: [30] 设置了格式 Shi, Pengfei 2023/11/22 11:29:00

字体颜色: 文字 1

第 9 页: [30] 设置了格式 Shi, Pengfei 2023/11/22 11:29:00

字体颜色: 文字 1

第 9 页: [30] 设置了格式 Shi, Pengfei 2023/11/22 11:29:00

字体颜色: 文字 1

第 9 页: [30] 设置了格式 Shi, Pengfei 2023/11/22 11:29:00

字体颜色: 文字 1

第 9 页: [30] 设置了格式 Shi, Pengfei 2023/11/22 11:29:00

字体颜色: 文字 1

第 9 页: [30] 设置了格式 Shi, Pengfei 2023/11/22 11:29:00

字体颜色: 文字 1

第 9 页: [30] 设置了格式 Shi, Pengfei 2023/11/22 11:29:00

字体颜色: 文字 1

第 9 页: [30] 设置了格式 Shi, Pengfei 2023/11/22 11:29:00

字体颜色: 文字 1

第 9 页: [30] 设置了格式 Shi, Pengfei 2023/11/22 11:29:00

字体颜色: 文字 1

第 9 页: [30] 设置了格式 Shi, Pengfei 2023/11/22 11:29:00

字体颜色: 文字 1

第 9 页: [30] 设置了格式 Shi, Pengfei 2023/11/22 11:29:00

字体颜色: 文字 1

第 9 页: [30] 设置了格式 Shi, Pengfei 2023/11/22 11:29:00

字体颜色: 文字 1

第 9 页: [30] 设置了格式 Shi, Pengfei 2023/11/22 11:29:00

字体颜色: 文字 1

第 9 页: [30] 设置了格式 Shi, Pengfei 2023/11/22 11:29:00

字体颜色: 文字 1

第 9 页: [30] 设置了格式 Shi, Pengfei 2023/11/22 11:29:00

字体颜色: 文字 1

第 9 页: [30] 设置了格式 Shi, Pengfei 2023/11/22 11:29:00

字体颜色: 文字 1

第 9 页: [30] 设置了格式 Shi, Pengfei 2023/11/22 11:29:00

字体颜色: 文字 1

第 9 页: [30] 设置了格式 Shi, Pengfei 2023/11/22 11:29:00

字体颜色: 文字 1

第 9 页: [30] 设置了格式　Shi, Pengfei　2023/11/22 11:29:00

字体颜色: 文字 1

第 9 页: [30] 设置了格式　Shi, Pengfei　2023/11/22 11:29:00

字体颜色: 文字 1

第 9 页: [30] 设置了格式　Shi, Pengfei　2023/11/22 11:29:00

字体颜色: 文字 1

第 9 页: [30] 设置了格式　Shi, Pengfei　2023/11/22 11:29:00

字体颜色: 文字 1

第 9 页: [30] 设置了格式　Shi, Pengfei　2023/11/22 11:29:00

字体颜色: 文字 1

第 9 页: [30] 设置了格式　Shi, Pengfei　2023/11/22 11:29:00

字体颜色: 文字 1

第 9 页: [30] 设置了格式　Shi, Pengfei　2023/11/22 11:29:00

字体颜色: 文字 1

第 9 页: [30] 设置了格式　Shi, Pengfei　2023/11/22 11:29:00

字体颜色: 文字 1

第 9 页: [30] 设置了格式　Shi, Pengfei　2023/11/22 11:29:00

字体颜色: 文字 1

第 9 页: [30] 设置了格式 Shi, Pengfei 2023/11/22 11:29:00

字体颜色: 文字 1

第 9 页: [30] 设置了格式 Shi, Pengfei 2023/11/22 11:29:00

字体颜色: 文字 1

第 9 页: [30] 设置了格式 Shi, Pengfei 2023/11/22 11:29:00

字体颜色: 文字 1

第 9 页: [31] 设置了格式 Shi, Pengfei 2023/11/22 11:29:00

字体颜色: 文字 1

第 9 页: [31] 设置了格式 Shi, Pengfei 2023/11/22 11:29:00

字体颜色: 文字 1

第 9 页: [31] 设置了格式 Shi, Pengfei 2023/11/22 11:29:00

字体颜色: 文字 1

第 9 页: [31] 设置了格式 Shi, Pengfei 2023/11/22 11:29:00

字体颜色: 文字 1

第 9 页: [31] 设置了格式 Shi, Pengfei 2023/11/22 11:29:00

字体颜色: 文字 1

第 9 页: [31] 设置了格式 Shi, Pengfei 2023/11/22 11:29:00

字体颜色: 文字 1

第 9 页: [31] 设置了格式 Shi, Pengfei 2023/11/22 11:29:00

字体颜色: 文字 1

第 9 页: [31] 设置了格式 Shi, Pengfei 2023/11/22 11:29:00

字体颜色: 文字 1

第 9 页: [31] 设置了格式 Shi, Pengfei 2023/11/22 11:29:00

字体颜色: 文字 1

第 9 页: [32] 设置了格式 Shi, Pengfei 2023/11/22 11:29:00

字体颜色: 文字 1

第 9 页: [32] 设置了格式 Shi, Pengfei 2023/11/22 11:29:00

字体颜色: 文字 1

第 9 页: [32] 设置了格式 Shi, Pengfei 2023/11/22 11:29:00

字体颜色: 文字 1

第 9 页: [32] 设置了格式 Shi, Pengfei 2023/11/22 11:29:00

字体颜色: 文字 1

第 9 页: [32] 设置了格式 Shi, Pengfei 2023/11/22 11:29:00

字体颜色: 文字 1

第 9 页: [32] 设置了格式 Shi, Pengfei 2023/11/22 11:29:00

字体颜色: 文字 1

第 9 页: [32] 设置了格式 Shi, Pengfei 2023/11/22 11:29:00

字体颜色: 文字 1

第 9 页: [32] 设置了格式 Shi, Pengfei 2023/11/22 11:29:00

字体颜色: 文字 1

第 9 页: [32] 设置了格式 Shi, Pengfei 2023/11/22 11:29:00

字体颜色: 文字 1

第 9 页: [32] 设置了格式 Shi, Pengfei 2023/11/22 11:29:00

字体颜色: 文字 1

第 9 页: [32] 设置了格式 Shi, Pengfei 2023/11/22 11:29:00

字体颜色: 文字 1

第 9 页: [32] 设置了格式 Shi, Pengfei 2023/11/22 11:29:00

字体颜色: 文字 1

第 9 页: [32] 设置了格式 Shi, Pengfei 2023/11/22 11:29:00

字体颜色: 文字 1

第 9 页: [32] 设置了格式 Shi, Pengfei 2023/11/22 11:29:00

字体颜色: 文字 1

第 9 页: [32] 设置了格式 Shi, Pengfei 2023/11/22 11:29:00

字体颜色: 文字 1

第 9 页: [32] 设置了格式 Shi, Pengfei 2023/11/22 11:29:00

字体颜色: 文字 1

第 9 页: [32] 设置了格式 Shi, Pengfei 2023/11/22 11:29:00

字体颜色: 文字 1

第 9 页: [32] 设置了格式 Shi, Pengfei 2023/11/22 11:29:00

字体颜色: 文字 1

第 9 页: [32] 设置了格式 Shi, Pengfei 2023/11/22 11:29:00

字体颜色: 文字 1

第 9 页: [32] 设置了格式 Shi, Pengfei 2023/11/22 11:29:00

字体颜色: 文字 1

第 9 页: [32] 设置了格式 Shi, Pengfei 2023/11/22 11:29:00

字体颜色: 文字 1

第 9 页: [32] 设置了格式 Shi, Pengfei 2023/11/22 11:29:00

字体颜色: 文字 1

第 9 页: [32] 设置了格式 Shi, Pengfei 2023/11/22 11:29:00

字体颜色: 文字 1

第 9 页: [32] 设置了格式 Shi, Pengfei 2023/11/22 11:29:00

字体颜色: 文字 1

第 9 页: [32] 设置了格式 Shi, Pengfei 2023/11/22 11:29:00

字体颜色: 文字 1

第 9 页: [32] 设置了格式 Shi, Pengfei 2023/11/22 11:29:00

字体颜色: 文字 1

第 9 页: [32] 设置了格式 Shi, Pengfei 2023/11/22 11:29:00

字体颜色: 文字 1

第 9 页: [32] 设置了格式 Shi, Pengfei 2023/11/22 11:29:00

字体颜色: 文字 1

第 9 页: [32] 设置了格式 Shi, Pengfei 2023/11/22 11:29:00

字体颜色: 文字 1

第 9 页: [32] 设置了格式 Shi, Pengfei 2023/11/22 11:29:00

字体颜色: 文字 1

第 9 页: [32] 设置了格式 Shi, Pengfei 2023/11/22 11:29:00

字体颜色: 文字 1

第 9 页: [32] 设置了格式 Shi, Pengfei 2023/11/22 11:29:00

字体颜色: 文字 1

第 9 页: [32] 设置了格式 Shi, Pengfei 2023/11/22 11:29:00

字体颜色: 文字 1

第 9 页: [32] 设置了格式 Shi, Pengfei 2023/11/22 11:29:00

字体颜色: 文字 1

第 9 页: [32] 设置了格式 Shi, Pengfei 2023/11/22 11:29:00

字体颜色: 文字 1

第 9 页: [32] 设置了格式 Shi, Pengfei 2023/11/22 11:29:00

字体颜色: 文字 1

第 9 页: [32] 设置了格式 Shi, Pengfei 2023/11/22 11:29:00

字体颜色: 文字 1

第 9 页: [32] 设置了格式 Shi, Pengfei 2023/11/22 11:29:00

字体颜色: 文字 1

第 9 页: [32] 设置了格式 Shi, Pengfei 2023/11/22 11:29:00

字体颜色: 文字 1

第 9 页: [32] 设置了格式 Shi, Pengfei 2023/11/22 11:29:00

字体颜色: 文字 1

第 9 页: [32] 设置了格式 Shi, Pengfei 2023/11/22 11:29:00

字体颜色: 文字 1

第 9 页: [32] 设置了格式 Shi, Pengfei 2023/11/22 11:29:00

字体颜色: 文字 1

第 9 页: [32] 设置了格式 Shi, Pengfei 2023/11/22 11:29:00

字体颜色: 文字 1

第 9 页: [32] 设置了格式 Shi, Pengfei 2023/11/22 11:29:00

字体颜色: 文字 1

第 9 页: [32] 设置了格式 Shi, Pengfei 2023/11/22 11:29:00

字体颜色: 文字 1

第 9 页: [32] 设置了格式 Shi, Pengfei 2023/11/22 11:29:00

字体颜色: 文字 1

第 9 页: [32] 设置了格式　Shi, Pengfei　2023/11/22 11:29:00

字体颜色: 文字 1

第 9 页: [32] 设置了格式　Shi, Pengfei　2023/11/22 11:29:00

字体颜色: 文字 1

第 9 页: [32] 设置了格式　Shi, Pengfei　2023/11/22 11:29:00

字体颜色: 文字 1

第 9 页: [32] 设置了格式　Shi, Pengfei　2023/11/22 11:29:00

字体颜色: 文字 1

第 9 页: [32] 设置了格式　Shi, Pengfei　2023/11/22 11:29:00

字体颜色: 文字 1

第 9 页: [32] 设置了格式　Shi, Pengfei　2023/11/22 11:29:00

字体颜色: 文字 1

第 9 页: [32] 设置了格式　Shi, Pengfei　2023/11/22 11:29:00

字体颜色: 文字 1

第 9 页: [32] 设置了格式　Shi, Pengfei　2023/11/22 11:29:00

字体颜色: 文字 1

第 9 页: [32] 设置了格式　Shi, Pengfei　2023/11/22 11:29:00

字体颜色: 文字 1

第 9 页: [32] 设置了格式 Shi, Pengfei 2023/11/22 11:29:00

字体颜色: 文字 1

第 9 页: [32] 设置了格式 Shi, Pengfei 2023/11/22 11:29:00

字体颜色: 文字 1

第 9 页: [32] 设置了格式 Shi, Pengfei 2023/11/22 11:29:00

字体颜色: 文字 1

第 9 页: [33] 设置了格式 Shi, Pengfei 2023/11/22 11:29:00

字体颜色: 文字 1

第 9 页: [33] 设置了格式 Shi, Pengfei 2023/11/22 11:29:00

字体颜色: 文字 1

第 9 页: [33] 设置了格式 Shi, Pengfei 2023/11/22 11:29:00

字体颜色: 文字 1

第 9 页: [33] 设置了格式 Shi, Pengfei 2023/11/22 11:29:00

字体颜色: 文字 1

第 9 页: [33] 设置了格式 Shi, Pengfei 2023/11/22 11:29:00

字体颜色: 文字 1

第 9 页: [33] 设置了格式 Shi, Pengfei 2023/11/22 11:29:00

字体颜色: 文字 1

第 9 页: [33] 设置了格式 Shi, Pengfei 2023/11/22 11:29:00

字体颜色: 文字 1

第 9 页: [33] 设置了格式 Shi, Pengfei 2023/11/22 11:29:00

字体颜色: 文字 1

第 9 页: [33] 设置了格式 Shi, Pengfei 2023/11/22 11:29:00

字体颜色: 文字 1

第 9 页: [33] 设置了格式 Shi, Pengfei 2023/11/22 11:29:00

字体颜色: 文字 1

第 9 页: [33] 设置了格式 Shi, Pengfei 2023/11/22 11:29:00

字体颜色: 文字 1

第 9 页: [33] 设置了格式 Shi, Pengfei 2023/11/22 11:29:00

字体颜色: 文字 1

第 9 页: [33] 设置了格式 Shi, Pengfei 2023/11/22 11:29:00

字体颜色: 文字 1

第 9 页: [33] 设置了格式 Shi, Pengfei 2023/11/22 11:29:00

字体颜色: 文字 1

第 9 页: [33] 设置了格式 Shi, Pengfei 2023/11/22 11:29:00

字体颜色: 文字 1

第 9 页: [33] 设置了格式 Shi, Pengfei 2023/11/22 11:29:00

字体颜色: 文字 1

第 9 页: [33] 设置了格式 Shi, Pengfei 2023/11/22 11:29:00

字体颜色: 文字 1

第 9 页: [33] 设置了格式 Shi, Pengfei 2023/11/22 11:29:00

字体颜色: 文字 1

第 9 页: [33] 设置了格式 Shi, Pengfei 2023/11/22 11:29:00

字体颜色: 文字 1

第 9 页: [33] 设置了格式 Shi, Pengfei 2023/11/22 11:29:00

字体颜色: 文字 1

第 9 页: [33] 设置了格式 Shi, Pengfei 2023/11/22 11:29:00

字体颜色: 文字 1

第 9 页: [33] 设置了格式 Shi, Pengfei 2023/11/22 11:29:00

字体颜色: 文字 1

第 9 页: [33] 设置了格式 Shi, Pengfei 2023/11/22 11:29:00

字体颜色: 文字 1

第 9 页: [34] 设置了格式 Shi, Pengfei 2023/11/22 11:29:00

字体颜色: 文字 1

第 9 页: [34] 设置了格式 Shi, Pengfei 2023/11/22 11:29:00

字体颜色: 文字 1

第 9 页: [34] 设置了格式 Shi, Pengfei 2023/11/22 11:29:00

字体颜色: 文字 1

第 9 页: [34] 设置了格式 Shi, Pengfei 2023/11/22 11:29:00

字体颜色: 文字 1

第 9 页: [35] 设置了格式 Shi, Pengfei 2023/11/22 11:29:00

字体颜色: 文字 1

第 9 页: [35] 设置了格式 Shi, Pengfei 2023/11/22 11:29:00

字体颜色: 文字 1

第 9 页: [35] 设置了格式 Shi, Pengfei 2023/11/22 11:29:00

字体颜色: 文字 1

第 9 页: [35] 设置了格式 Shi, Pengfei 2023/11/22 11:29:00

字体颜色: 文字 1

第 9 页: [35] 设置了格式 Shi, Pengfei 2023/11/22 11:29:00

字体颜色: 文字 1

第 9 页: [36] 设置了格式 Shi, Pengfei 2023/11/22 11:29:00

字体颜色: 文字 1

第 9 页: [36] 设置了格式 Shi, Pengfei 2023/11/22 11:29:00

字体颜色: 文字 1

第 9 页: [36] 设置了格式 Shi, Pengfei 2023/11/22 11:29:00

字体颜色: 文字 1

第 9 页: [36] 设置了格式 Shi, Pengfei 2023/11/22 11:29:00

字体颜色: 文字 1

第 9 页: [37] 设置了格式 Shi, Pengfei 2023/11/22 11:29:00

字体颜色: 文字 1

第 9 页: [37] 设置了格式 Shi, Pengfei 2023/11/22 11:29:00

字体颜色: 文字 1

第 9 页: [37] 设置了格式 Shi, Pengfei 2023/11/22 11:29:00

字体颜色: 文字 1

第 9 页: [37] 设置了格式　Shi, Pengfei　2023/11/22 11:29:00

字体颜色: 文字 1

第 9 页: [37] 设置了格式　Shi, Pengfei　2023/11/22 11:29:00

字体颜色: 文字 1

第 9 页: [37] 设置了格式　Shi, Pengfei　2023/11/22 11:29:00

字体颜色: 文字 1

第 9 页: [37] 设置了格式　Shi, Pengfei　2023/11/22 11:29:00

字体颜色: 文字 1

第 9 页: [37] 设置了格式　Shi, Pengfei　2023/11/22 11:29:00

字体颜色: 文字 1

第 9 页: [37] 设置了格式　Shi, Pengfei　2023/11/22 11:29:00

字体颜色: 文字 1

第 9 页: [37] 设置了格式　Shi, Pengfei　2023/11/22 11:29:00

字体颜色: 文字 1

第 9 页: [37] 设置了格式　Shi, Pengfei　2023/11/22 11:29:00

字体颜色: 文字 1

第 9 页: [37] 设置了格式　Shi, Pengfei　2023/11/22 11:29:00

字体颜色: 文字 1

第 9 页: [37] 设置了格式　Shi, Pengfei　2023/11/22 11:29:00

字体颜色: 文字 1

第 9 页: [37] 设置了格式　Shi, Pengfei　2023/11/22 11:29:00

字体颜色: 文字 1

第 9 页: [37] 设置了格式　Shi, Pengfei　2023/11/22 11:29:00

字体颜色: 文字 1

第 9 页: [37] 设置了格式　Shi, Pengfei　2023/11/22 11:29:00

字体颜色: 文字 1

第 9 页: [37] 设置了格式　Shi, Pengfei　2023/11/22 11:29:00

字体颜色: 文字 1

第 9 页: [37] 设置了格式　Shi, Pengfei　2023/11/22 11:29:00

字体颜色: 文字 1

第 9 页: [37] 设置了格式　Shi, Pengfei　2023/11/22 11:29:00

字体颜色: 文字 1

第 9 页: [37] 设置了格式　Shi, Pengfei　2023/11/22 11:29:00

字体颜色: 文字 1

第 9 页: [37] 设置了格式 Shi, Pengfei 2023/11/22 11:29:00

字体颜色: 文字 1

第 9 页: [37] 设置了格式 Shi, Pengfei 2023/11/22 11:29:00

字体颜色: 文字 1

第 9 页: [37] 设置了格式 Shi, Pengfei 2023/11/22 11:29:00

字体颜色: 文字 1

第 9 页: [37] 设置了格式 Shi, Pengfei 2023/11/22 11:29:00

字体颜色: 文字 1

第 9 页: [37] 设置了格式 Shi, Pengfei 2023/11/22 11:29:00

字体颜色: 文字 1

第 9 页: [37] 设置了格式 Shi, Pengfei 2023/11/22 11:29:00

字体颜色: 文字 1

第 9 页: [37] 设置了格式 Shi, Pengfei 2023/11/22 11:29:00

字体颜色: 文字 1

第 9 页: [37] 设置了格式 Shi, Pengfei 2023/11/22 11:29:00

字体颜色: 文字 1

第 9 页: [37] 设置了格式 Shi, Pengfei 2023/11/22 11:29:00

字体颜色: 文字 1

第 9 页: [37] 设置了格式 Shi, Pengfei 2023/11/22 11:29:00

字体颜色: 文字 1

第 9 页: [37] 设置了格式 Shi, Pengfei 2023/11/22 11:29:00

字体颜色: 文字 1

第 9 页: [37] 设置了格式 Shi, Pengfei 2023/11/22 11:29:00

字体颜色: 文字 1

第 9 页: [37] 设置了格式 Shi, Pengfei 2023/11/22 11:29:00

字体颜色: 文字 1

第 9 页: [37] 设置了格式 Shi, Pengfei 2023/11/22 11:29:00

字体颜色: 文字 1

第 9 页: [37] 设置了格式 Shi, Pengfei 2023/11/22 11:29:00

字体颜色: 文字 1

第 9 页: [37] 设置了格式 Shi, Pengfei 2023/11/22 11:29:00

字体颜色: 文字 1

第 9 页: [37] 设置了格式 Shi, Pengfei 2023/11/22 11:29:00

字体颜色: 文字 1

第 9 页: [37] 设置了格式 Shi, Pengfei 2023/11/22 11:29:00

字体颜色: 文字 1

第 9 页: [38] 设置了格式 Shi, Pengfei 2023/11/22 11:29:00

字体颜色: 文字 1

第 9 页: [38] 设置了格式 Shi, Pengfei 2023/11/22 11:29:00

字体颜色: 文字 1

第 9 页: [38] 设置了格式 Shi, Pengfei 2023/11/22 11:29:00

字体颜色: 文字 1

第 9 页: [38] 设置了格式 Shi, Pengfei 2023/11/22 11:29:00

字体颜色: 文字 1

第 9 页: [39] 设置了格式 Shi, Pengfei 2023/11/22 11:29:00

字体颜色: 文字 1

第 9 页: [39] 设置了格式 Shi, Pengfei 2023/11/22 11:29:00

字体颜色: 文字 1

第 9 页: [39] 设置了格式 Shi, Pengfei 2023/11/22 11:29:00

字体颜色: 文字 1

第 9 页: [39] 设置了格式 Shi, Pengfei 2023/11/22 11:29:00

字体颜色: 文字 1

第 9 页: [39] 设置了格式 Shi, Pengfei 2023/11/22 11:29:00

字体颜色: 文字 1

第 9 页: [40] 删除了 Shi, Pengfei 2023/10/10 16:34:00

第 9 页: [40] 删除了 Shi, Pengfei 2023/10/10 16:34:00

第 9 页: [40] 删除了 Shi, Pengfei 2023/10/10 16:34:00